



MASTER 2 RESEARCH REPORT

DISC

**IMAGE RESTORATION BY
INPAINTING METHODS
APPLIED TO CT RECONSTRUCTION.**

MARCOS VARGAS

(B.Sc. and Degree in Electronics Eng.)

DISC/LITT/Rév. 1

September 2012

Tuteur Entreprise: Mr Marius COSTIN (CEA)

Tuteur Ecole: Mr Olivier BERNARD (INSA-Lyon)

Stage du lundi 2 avril 2012 (S14) au vendredi 31 août 2012 (S35). CEA-Saclay, DRT-LIST-DISC-LITT.

Titre : Restauration d'image par méthodes de type "inpainting" appliquée à la reconstruction tomographique	DISC/ 11 RT 000
Auteur : MARCOS VARGAS	09 2012
CO-AUTEURS: MARIUS COSTIN	Revision : 1
PROJET : STAGE M2R	Nombre de pages: 49

Documents Associés

Résumé :

Inpainting numériques est l'art de remplir les pièces perdues ou détériorées des images ou des vidéos dans un format qui n'est pas perceptible par un observateur ordinaire. Artefact est une erreur dans la représentation de l'information introduite par l'équipement ou la technique concernés. La réduction d'artefact, est considéré comme un sujet crucial dans la recherche et le développement de CT. Notre approche est d'obtenir une réduction des artefacts métalliques (MAR), en comparant les résultats de 2D Inpainting dans les domaines de projection et sinogramme. Nos images CT viennent de: CIVA (simulation), SkyScan2011, PerkinElmer (expérimental). Tout d'abord, nous avons testé huit algorithmes de Inpainting: Total Variation (TV), Curvature Driven Diffusion (CDD), Mean Curvature Diffusion (MCD), Euler's Elastica, Morphologic Rotation Invariant (MRI), Fast Marching Method (FMM), Anisotropic Diffusion-Based (AdB) and Exemplar-Based (ExB). Ensuite, nous avons validé nos résultats en utilisant l'erreur quadratique moyenne (MSE), pic du rapport signal sur bruit (PSNR) et le multi-échelle indice de similarité structurelle (MS-SSIM). Les résultats ont été comparés entre eux en tenant compte: le temps et les trois paramètres de la qualité d'image mentionnés. Enfin, nos expériences ont démontré que nos deux meilleurs résultats de qualité pour MAR ont été obtenus par CDD et ExB, pour nos images expérimentales dans le domaine de projection. Les résultats dans le domaine de sinogramme ne sont que qualitatives.

Mots-clés: Inpainting, Artifact, x-ray CT, TV, CDD, Fast Marching, PDE, Exemplar-Based.

1	August 30, 2012	MARCOS VARGAS	MARIUS COSTIN			
0	August 07, 2012	MARCOS VARGAS	MARIUS COSTIN			
Rév.	Date	Rédacteur	Vérificateur			

Les informations contenues dans ce document ne sont pas destinées à la publication
Il ne peut en être fait état sans autorisation expresse du Commissariat à l'Energie Atomique




  LABORATOIRE D'INTEGRATION DES SYSTEMES ET DES TECHNOLOGIES	Image restoration by inpainting methods applied to CT reconstruction	Réf : DISC/LITT /11 RT000	3
		DATE: 04 09 2012	49
DISC/LITT	Marcos VARGAS	 Révision	1

Image restoration by inpainting methods applied to CT reconstruction.
by
Marcos Vargas

Submitted to Institut National des Sciences Appliquées de Lyon (INSA-Lyon)
on September 04, 2012, in partial fulfillment of the
requirements for the degree of

Master EEAP (Electronique Electrotechnique Automatique Procédés) - Parcours Systèmes et Images

Abstract

Digital inpainting is the art of filling in lost or deteriorated parts of images or videos in a form that is not noticeable by an ordinary observer. Artifact is any error in the information representation introduced by the involved equipment or technique. Artifact Reduction, is considered a critical topic in x-ray CT research and development. Our approach is to get a metal artifact reduction (MAR), by comparing 2D inpainting results in the projection and sinogram domains. Our CT images came from: CIVA (simulation), SkyScan2011, PerkinElmer (experimental). First, we tested eight inpainting algorithms: Total Variation (TV), Curvature Driven Diffusion (CDD), Mean Curvature Diffusion (MCD), Euler's Elastica, Morphologic Rotation Invariant (MRI), Fast Marching Method (FMM), Anisotropic Diffusion-Based (AdB) and Exemplar-Based (ExB). Then, we validated our results using mean squared error (MSE), peak signal-to-noise ratio (PSNR) and Multi-Scale Structural Similarity Index (MS-SSIM). Results were compared among them considering: time and the three image quality assessments mentioned. Finally, our experiments demonstrated that our two best MAR quality results were achieved by CDD and ExB, for our experimental images in the projection domain. The results in the sinogram domain were only qualitative.

Keywords: Inpainting, Artifact, x-ray CT, TV, CDD, Fast Marching, PDE, Exemplar-Based.

Résumé

Inpainting numériques est l'art de remplir les pièces perdues ou détériorées des images ou des vidéos dans un format qui n'est pas perceptible par un observateur ordinaire. Artefact est une erreur dans la représentation de l'information introduite par l'équipement ou la technique concernés. La réduction d'artefact, est considéré comme un sujet crucial dans la recherche et le développement de CT. Notre approche est d'obtenir une réduction des artéfacts métalliques (MAR), en comparant les résultats de 2D Inpainting dans les domaines de projection et sinogramme. Nos images CT viennent de: CIVA (simulation), SkyScan2011, PerkinElmer (expérimental). Tout d'abord, nous avons testé huit algorithmes de Inpainting: Total Variation (TV), Curvature Driven Diffusion (CDD), Mean Curvature Diffusion (MCD), Euler's Elastica, Morphologic Rotation Invariant (MRI), Fast Marching Method (FMM), Anisotropic Diffusion-Based (AdB) and Exemplar-Based (ExB). Ensuite, nous avons validé nos résultats en utilisant l'erreur quadratique moyenne (MSE), pic du rapport signal sur bruit (PSNR) et le multi-échelle indice de similarité structurelle (MS-SSIM). Les résultats ont été comparés entre eux en tenant compte: le temps et les trois paramètres de la qualité d'image mentionnés. Enfin, nos expériences ont démontré que nos deux meilleurs résultats de qualité pour MAR ont été obtenus par CDD et ExB, pour nos images expérimentales dans le domaine de projection. Les résultats dans le domaine de sinogramme ne sont que qualitatives.

Mots-clés: Inpainting, Artifact, x-ray CT, TV, CDD, Fast Marching, PDE, Exemplar-Based.



Professional Supervisor: Marius COSTIN (CEA)

Title: Research Scientist

University Supervisor: Olivier BERNARD (INSA-Lyon)

Title: Maître de Conférences des Universités

September 04, 2012

 list LABORATOIRE D'INTEGRATION DES SYSTEMES ET DES TECHNOLOGIES	Image restoration by inpainting methods applied to CT reconstruction	Réf : DISC/LITT /11 RT000	4
		DATE: 04 09 2012	49
DISC/LITT	Marcos VARGAS	 Révision	1

“To my Family...”

Acknowledgements



I would like to thanks Marius COSTIN, my internship supervisor for all the continuous help, patience and guidance throughout this research topic. He has given me both guidelines to do research in and insight to help narrow and contain them. He has contributed with numerous unique ideas to the research that it is untoward that I was only able to pursue a small number of them.

I would like to thanks to my Family for their encouragement and for their support and help across this time. Also thanks to Prof. Simon Masnou for sharing a selected material, from his conference on Inpainting Methods [1].


“Think Analog, Act Digital”¹




Michael Unser

¹ Plenary talk at the Seventh Biennial Conference, 2004 International Conference on Signal Processing and Communications (SPCOM'04).

 list LABORATOIRE D'INTEGRATION DES SYSTEMES ET DES TECHNOLOGIES	Image restoration by inpainting methods applied to CT reconstruction	Réf : DISC/LITT /11 RT000	5
		DATE: 04 09 2012	49
DISC/LITT	Marcos VARGAS	 Révision	1

Contents

ABSTRACT 	3
ACKNOWLEDGEMENTS	4
LIST OF APPENDICES	6
GLOSSARY	6
LIST OF FIGURES	7
1. INTRODUCTION	9
2. CONTEXT	11
2.1. CT Reconstruction Techniques Classification	12
2.2. Artifacts Classification	12
2.3. Metal Artifact Reduction (MAR)	13
3. STATE OF THE ART (SOTA)	14
3.1. 2D Digital Inpainting Methods	14
3.2. 2D Digital Inpainting Software	15
3.3. Metal Artifact Reduction (MAR)	15
3.4. Conclusion on our SOTA	15
4. METHODS	16
4.1. Fast Marching Method (FMM) [6]	16
4.2. Total Variation (TV)	18
4.2.1. Naïve Rudin [9] [10]	18
4.2.2. Curvature Driven Diffusion (CDD) [11]	19
4.2.3. Mean Curvature Diffusion (MCD) [12]	21
4.2.4. Euler's Elastica: CDD and MCD Combined [13]	21
4.2.5. Morphologically Rotation Invariant (MRI) [16]	23
4.2.6. Conclusion on TV Inpainting Families	23
4.3. Anisotropic Diffusion-Based (AdB) [17]	23
4.4. Exemplar-Based (ExB) [18]	25
4.5. Conclusion	26
5. RESULTS AND DISCUSSION	27
5.1. Materials	27
5.2. Methodology	29
5.2.1. Mask	29
5.2.2. Image Quality Assessment	30
5.3. Evaluation on:	30
5.3.1. Simple Synthetic Images	30
5.3.2. A CT Realistic Synthetic Image from CIVA (noiseless) in Projection	31
5.3.3. CT Real Images from SkyScan2011 and PerkinElmer (noisy) in Projection.	33
5.4. Algorithm Optimization and Test on Sinograms	35
5.4.1. Optimization for Fast Inpainting Execution	35
5.4.1. Semi-automatic Mask Creation	36
5.4.2. Evaluation on a CT Realistic Synthetic Image from CIVA (noiseless)	36
5.4.3. Evaluation on a CT Real Image from SkyScan2011 (noisy)	37
5.5. Choice of the Adapted Algorithm	38
5.6. Validation on Simple Synthetic Images (noiseless)	39
5.7. Validation on a CT Real Image from PerkinElmer (noisy) in Projection	40
5.1. Validation on a CT Realistic Synthetic Image (noiseless) in Sinogram	40
6. CONCLUSIONS AND DIRECTIONS FOR FUTURE WORK	41
BIBLIOGRAPHY	43

  LABORATOIRE D'INTEGRATION DES SYSTEMES ET DES TECHNOLOGIES	Image restoration by inpainting methods applied to CT reconstruction	Réf : DISC/LITT /11 RT000	6
		DATE: 04 09 2012	49
DISC/LITT	Marcos VARGAS	 Révision	1

List of Appendices

Appendix 1

CEA: Atomic Energy and Alternative Energies Commission 46

Appendix 2




Level Set Methods (LSMs) vs Fast Marching Methods (FMMs): Similarities & Differences. 47

Appendix 3

FMM and ExB. UML classes used. 48

Glossary

Abbreviation	Description
BMP or DIB	Bitmap Image File
CDD	Curvature Driven Diffusions
CT	X-ray Computed Tomography
DQE	Detective Quantum Efficiency
<i>eI</i>	'evolving Interface' (eI) = Interface
FBP	Filtered Back-Projection (Algorithm)
FMM	Fast Marching Method
GSL	GNU Scientific Library
GUI	Graphical User Interface
Isophotes	Lines of equal gray value
MAR	Metal Artifacts Reduction
MPR	Metal Projection Region
MS-SSIM	Multi-Scale Structural Similarity Index
MTF	Modulation Transfer Function
NDT	Non-Destructive Testing
PDE	Partial Differential Equation
PSNR [dB]	Peak signal-to-noise ratio expressed in dB
ROI	Region Of Interest
SOTA	State of the Art
TIFF	Tagged Image File Format
TV	Total Variation Method

  LABORATOIRE D'INTEGRATION DES SYSTEMES ET DES TECHNOLOGIES	Image restoration by inpainting methods applied to CT reconstruction	Réf : DISC/LITT /11 RT000	7
		DATE: 04 09 2012	49
DISC/LITT	Marcos VARGAS	 Révision	1

List of Figures

Figure 1-1. Inpainting general concept: (a) CT real image from SkyScan (noisy sinogram), (b) the mask, defines the unwanted part in white, (c) result after using the CDD inpainting algorithm (see section 5.4.3 for details).9	
Figure 2-1. Sketch of the CT process: (a) acquisition of the projections, (b) sinogram and (c) reconstructed image [3].	11
Figure 2-2. Part of the CT Reconstruction Techniques Classification.	12
Figure 2-4. 2D Artifacts: Origin-Based Classification (internal images taken from [3]).	13
Figure 2-4. Metal Artifacts: Mainly phenomena (the internal image comes from [4])	13
Figure 3-1. Numbers of retrieved papers during 1991–2012 with the searching rules mentioned in each legend (a) Inpainting and CT (b) Inpainting Methods. The polynomial fittings show that there is an 75% increment yearly for the former, while a 70% increment for the latter. Note that the numbers for 2012 are incomplete.	14
Figure 3-2. (a) MAR SOTA. Flow charts of some iterative CT algorithms from (b) Y. Li et al. [4] (c)E. Meyer et al. [5]	15
Figure 4-1. General Classification of Methods in 2D Digital Inpainting.	16
Figure 4-2. FMM: (a) the gray part is the zone to inpaint[6], (b) zoom for gradient in the border[6], (c) equation [6].	17
Figure 4-3. FMM Context (*FMMs: Optimal way to solve Hamilton-Jacobi Equation.)	17
Figure 4-4. TV Context.	18
Figure 4-5. (a) Naïve Rudin TV Inpainting model (b) Input [10] (c) Output [10].	18
Figure 4-6. Naïve Rudin TV disadvantage [11].	19
Figure 4-7. CDD: Connectivity Principle (a)Input (b)Mask (c) Output [11] (i.e. using straight lines for circular arcs)	20
Figure 4-8. Divergence Operator: Grid of a given image, around pixel (0,0) [inspired on [11]]	20
Figure 4-9. MCD, mathematical definition.	21
Figure 4-10. (a) Comparative table on the implemented ideas [12] (b) Result of the algorithm [12]	21
Figure 4-11. (a) Tangent and Normal (b) Euler's Elastica vs TV. [14]	21
Figure 4-12. On the left side an x-half-point and on the right side a y-half-point [15].	22
Figure 4-13. Naïve Rudin vs Euler's Elastica. Rows (1): Circle problem, (2): Broken bars problem. Columns (a) Images with different sizes for the occluding noisy squares, (b) mask, (c) Rudin result, (d) Euler's Elastica result. [15]	22
Figure 4-14. TV Inpainting Family	23
Figure 4-15. AdB inpainting technique, where the image in the center is the mask defined by the user[17].	24
Figure 4-16. Flow Diagram of the AdB algorithm.	24
Figure 4-17. (a) ExB Basic Diagram [18] (b) ExB formula.	25
Figure 4-18. Flow Diagram of the ExB algorithm.	26
Figure 4-19. Our general 2D digital inpainting methods classification.	26
Figure 5-1. (a)(b)(c) Simple geometric forms; (d) 24-bit Bitmap profile of c (simple version of Figure 5-2).	27
Figure 5-2. CIVVA, (a) scene and CT setup, (b) 16-bit TIFF profile, (c) tomography displacement [19].	28






 list LABORATOIRE D'INTEGRATION DES SYSTEMES ET DES TECHNOLOGIES	Image restoration by inpainting methods applied to CT reconstruction	Réf : DISC/LITT /11 RT000	8
		DATE: 04 09 2012	49
DISC/LITT	Marcos VARGAS	 Révision	1

Figure 5-3. The Nano-CT device SkyScan2011:(a) External view, (b)Internal view[20],(c) Projection image @ 0° [20].	28
Figure 5-4. PerkinElmer device:(a) external view (b) material position (c) projection image @ 0°.	29
Figure 5-5. Our 3-step planning, an insight on our evaluation techniques.	29
Figure 5-6. Simple Synthetic images (509 x 506 px.) created for initial tests: (a) image with white parts representing lost information, (b) mask, (c) FMM, 25s. 50k iterations. (d) AdB, 62517.4 s. 60.3k iterations (e) CDD, 76.45 s.	30
Figure 5-7. Overview of the 2 different domains: Projection and Sinogram.	31
Figure 5-8. Legend for the next results.	31
Figure 5-9. Test on Noiseless Images (CIVA). Internal images were cropped to 103 x 103 for visibility.	33
Figure 5-10. Test on Noisy Images (SkyScan2011). Internal images were cropped to 106 x 69 for visibility.	34
Figure 5-11. Test on Noisy Images (PerkinElmer). Internal images were cropped to 82 x 85 for visibility.	35
Figure 5-12. Optimization Results.	35
Figure 5-13. Semi-automatic Mask Creation (used in Figure 5-14).	36
Figure 5-14. Test on Noiseless Sinogram (CIVA). Internal images were cropped to 51 x 72 for visibility.	37
Figure 5-15. Test on experimental Sinogram. Internal images were cropped to 128 x 36 for visibility.	38
Figure 5-16. Radar chart of the 04 best results of Figure 5-9 (right), detailed table (left).	38
Figure 5-17. Radar chart of the 04 best results of Figure 5-10 (right), detailed table (left).	38
Figure 5-18. Radar chart of the 04 best results of Figure 5-11 (right), detailed table (left).	39
Figure 5-19. Radar chart of the 03 best results of Figure 5-14 (right), detailed table (left).	39
Figure 5-20. Simple Synthetic Image: (a) Region to inpaint zoomed, (b)mask. Zoomed regions of the comparative images using: (c) TV, (d) CDD, (e) Euler's Elastica and (f) AdB.	39
Figure 5-21. Problem in inpainting circular zones. Zoomed comparative images of PerkinElmer (Figure 5-11) using:	40
Figure 5-22. Particular case in the Sinogram domain. Internal images were cropped to 94 x 67 for visibility.	40

  LABORATOIRE D'INTEGRATION DES SYSTEMES ET DES TECHNOLOGIES	Image restoration by inpainting methods applied to CT reconstruction	Réf : DISC/LITT /11 RT000	9
		DATE: 04 09 2012	49
DISC/LITT	Marcos VARGAS	 Révision	1

Chapter 1

Introduction

Inpainting is an “artistic way of saying image interpolation”², also it can be seen as a “likely” reconstruction of a missing domain (scratched or undesirable) in a 2D/3D image or a sequence. Usually the parts to get inpainted are identified by the user, in Figure 1-1 b) the white regions indicate such missing information areas, the so-called *mask*. In the literature the following terms are also used as a synonym of inpainting: filling-in, completion, disocclusion and error concealment.

2D inpainting based restoration methods have been developed for image restoration in computer vision. In the x-ray imaging framework, x-ray computed tomography (CT) is a non-invasive imaging technique that allows to examine slices of an object without damaging it. For medical imaging, non-destructive testing or material science, these methods can be applied for different purposes, such as artifacts reduction due to high contrast components in the object, missing data or as a method to reduce the dose delivered to the human body during exam by artificial data completion for example.

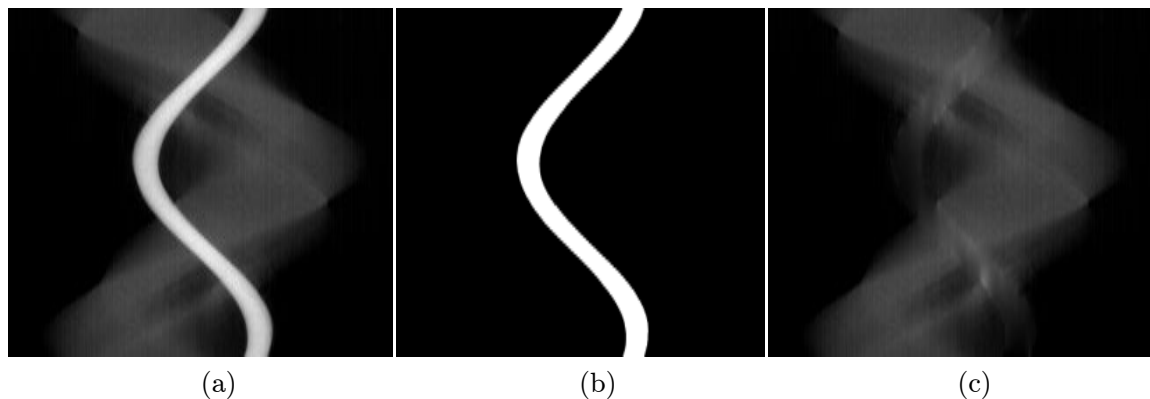





Figure 1-1. Inpainting general concept: (a) CT real image from SkyScan (noisy sinogram), (b) the mask, defines the unwanted part in white, (c) result after using the CDD inpainting algorithm (see section 5.4.3 for details).

² As first used in IP by Bertalmio et al (SIGGRAPH, 2000)

  LABORATOIRE D'INTEGRATION DES SYSTEMES ET DES TECHNOLOGIES	Image restoration by inpainting methods applied to CT reconstruction	Réf : DISC/LITT /11 RT000	10
		DATE: 04 09 2012	49
DISC/LITT	Marcos VARGAS	 Révision	1

Objective

To focus on 2D digital inpainting methods for metal artifact correction on x-ray and CT images, in particular streak artifacts, i.e. the correction for very high attenuation regions, e.g. metal artifacts.

General Tools




All the next software mentioned herein have been used under Windows 7 Enterprise SP1. The coding platform was Microsoft Visual Studio 2010 Professional (C++). The sketches and figures were made with CorelDRAW X5 (<http://www.corel.com/corel/>). We used Fiji (<http://fiji.sc/wiki/index.php/Fiji>) for some images calculation and other enhancements, and ImageJ's plugging (<http://rsb.info.nih.gov/ij/>) for Image Quality assessment. For opening TIFF images we used Irfan View (www.irfanview.com) and for getting simply its properties we used AsTiffTagViewer (<http://www.awaresystems.be/imaging/tiff/astifftagviewer.html>).

For the reference management software, we used Qiqqa (<http://www.qiqqa.com/>) that allowed us to work with thousands of papers within annotations, tags and comments using the internet cloud-based Qiqqa Web Libraries. For the UML part, we found that StarUML (<http://staruml.sourceforge.net/en/>) was the most adapted.

For a Unix-like environment and command-line interface for Windows 7, we used Cygwin (<http://cygwin.com/>); and as a native software port of the GNU Compiler Collection (GCC) and GNU Binutils, we used MinGW(<http://mingw.org/>). Finally, some algorithms where tested under Mathematica 8.0 and MATLAB R2010b.

Chapters Overview

The rest of the manuscript is structured as follows. **Chapter 2: Context**, describes our objective in the framework of artifact correction. **Chapter 3: State of the Art**, provides the 10-year tendency on inpainting methods. **Chapter 4: Methods**, provides diagrams for summing up all the different classification of inpainting methods. **Chapter 5: Results and Discussion**, provides the tests made on both CT simulated and CT experimental data, and through image quality assessment we discuss and present our choices for adapted algorithms to our problem. **Chapter 6: Conclusions and Directions for Future Work**, provides a summary of our work, final remarks and some perspectives. All the chapters are made as modular as possible, i.e. some of them end with a conclusion part, re-usable as the ideas are developed throughout this report.

  LABORATOIRE D'INTEGRATION DES SYSTEMES ET DES TECHNOLOGIES	Image restoration by inpainting methods applied to CT reconstruction	Réf : DISC/LITT /11 RT000	11
		DATE: 04 09 2012	49
DISC/LITT	Marcos VARGAS	 Révision	1

Chapter 2

Context

Artifacts (or *Artefacts*³) are misrepresentations (errors in the reconstruction) of structures seen in images produced by modalities such as ultrasonography, CT or MRI. Artifacts are introduced by a technique and/or technology. They can critically corrupt the reconstructed images, occasionally to the point of making them diagnostically useless. In order to optimize image quality, it is compulsory to understand why artifacts occur and how they can be prevented or suppressed, i.e. in the big picture problem be aware which are the frontiers between *hardware-based artifacts* (physics-based artifacts, object-based artifacts, scanner-based artifacts) and *software-based artifacts* (helical and multi-slice artifacts); so that the digital image restoration, in this case inpainting, could consider those constraints in their methods. CT provides 3D structural information of an object, the desired images are computed from a set of X-ray projections of the object at different orientations.

All the X-rays set measured with the detector at a given angular location forms a discrete projection. We have two options, or the source and the detector rotate around the sample, or only the sample rotates. Several projections can be recorded at different angular positions. The collection of these measurements consecutively ordered with the angular position is called sinogram. “The main idea of the CT reconstruction is to recover the function that maps the linear attenuation coefficients for all the pixels of the imaged object, from a sinogram” [2]. Figure 2-1 shows an example of a CT acquisition, the resulting sinogram and the reconstructed image.

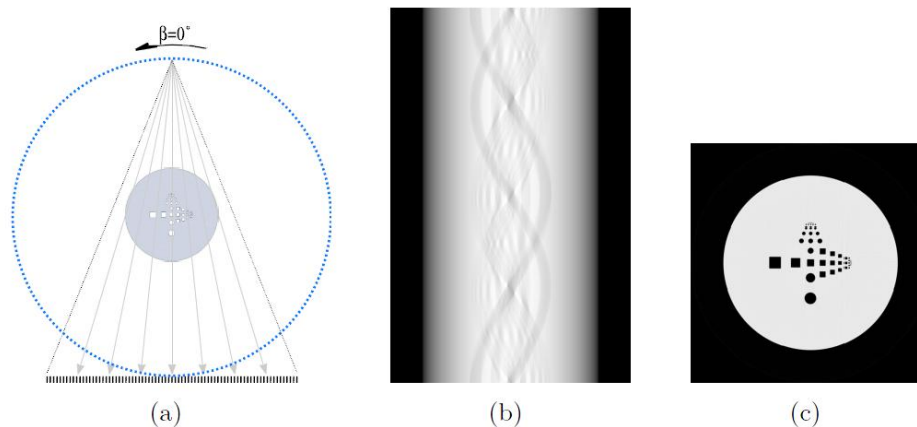





Figure 2-1. Sketch of the CT process: (a) acquisition of the projections, (b) sinogram and (c) reconstructed image [3].

³ In British English, *artefact* is the main spelling and *artifact* a minor variant (Oxford English Dictionary, *artefact*). In American English, *artifact* is the usual spelling. Canadians prefer *artifact* and Australians *artefact*, according to their respective dictionaries. *Artefact* reflects *Arte-fact(um)*, the Latin source. (Oxford English Dictionary. Oxford, England: Oxford University Press. March 2009.)

  LABORATOIRE D'INTEGRATION DES SYSTEMES ET DES TECHNOLOGIES	Image restoration by inpainting methods applied to CT reconstruction	Réf : DISC/LITT /11 RT000	12
		DATE: 04 09 2012	49
DISC/LITT	Marcos VARGAS	 Révision	1

2.1. CT Reconstruction Techniques Classification

The tomographic images or 'slides' of specific areas of an object are created as follow. An object is x-rayed from several angles (around an axis of rotation), producing a set of x-ray projections. Then we take the same row of the different projections by superposing them, the so-called *sinogram*. Each sinogram row corresponds to an x-ray projection at one specific angle. CT reconstruction calculates from this set of 1D sinograms a reconstructed 2D image, a slice through the examined object internal structure. A general CT reconstruction techniques classification can be seen in Figure 2-2.

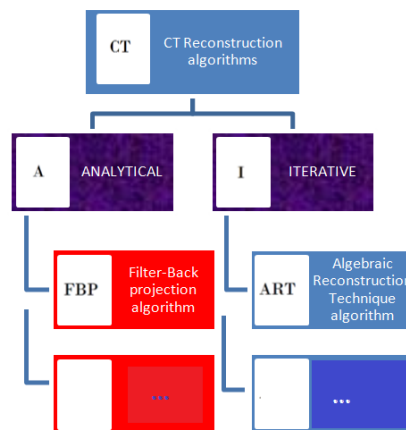
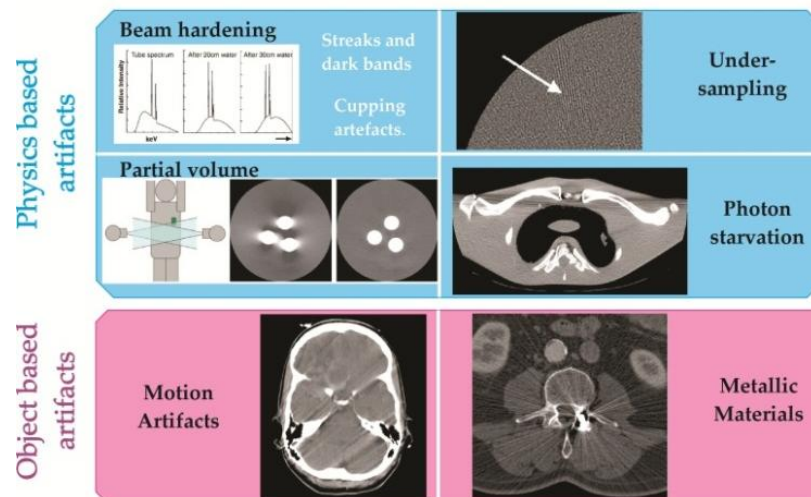




Figure 2-2. Part of the CT Reconstruction Techniques Classification.

2.2. Artifacts Classification

In CT several types of artifact may affect the images and they have different origin. The artifacts can be classified as: physics-based, object-based, scanner-based or helical and multi-slice artifacts. Each of them could have subdivisions, as it is the case of the object-based artifacts. Inside the object-based artifacts, we see the case of metallic materials or metal artifact. We sketched a classification of the 2D artifact environment according to [2], synthesized in:



 list LABORATOIRE D'INTEGRATION DES SYSTEMES ET DES TECHNOLOGIES	Image restoration by inpainting methods applied to CT reconstruction	Réf : DISC/LITT /11 RT000	13
		DATE: 04 09 2012	49
DISC/LITT	Marcos VARGAS	 Révision	1

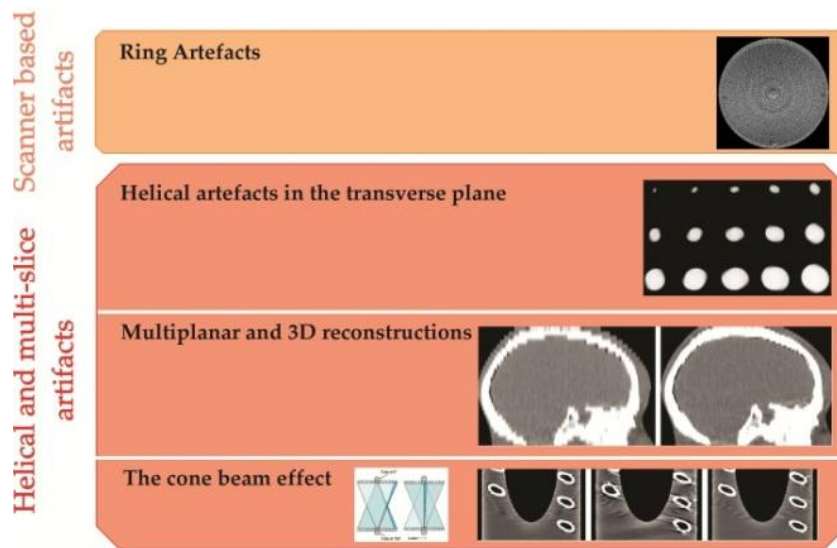


Figure 2-3. 2D Artifacts: Origin-Based Classification (internal images taken from [3]).

2.3. Metal Artifact Reduction (MAR)

Metal artifact is a degradation of the image quality due to the presence of inserts of very attenuating material such as metals (Figure 2-3). We observed them, at the reconstructed images, as streak. Our goal is to inpaint the metal artifacts in the reconstructed CT images. Figure 2-4 shows the interaction of different phenomena that creates a metal artifact.

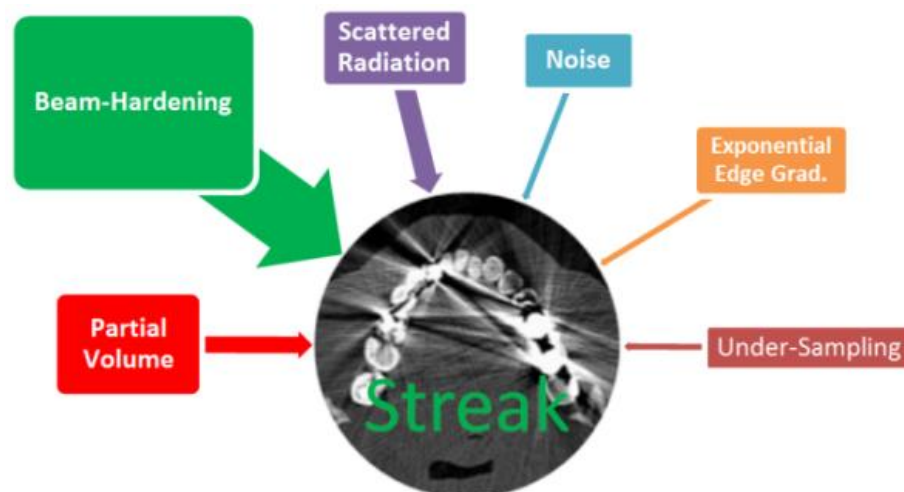





Figure 2-4. Metal Artifacts: Mainly phenomena (the internal image comes from [4])

  LABORATOIRE D'INTEGRATION DES SYSTEMES ET DES TECHNOLOGIES	Image restoration by inpainting methods applied to CT reconstruction	Réf : DISC/LITT /11 RT000	14
		DATE: 04 09 2012	49
DISC/LITT	Marcos VARGAS	 Révision	1

Chapter 3

State of the Art (SOTA)

3.1. 2D Digital Inpainting Methods

We analyzed the tendencies in inpainting and its relation within the CT context (Figure 3-1). Our quantitative literature analysis methodology was to examine the *ISI Web of Knowledge*⁴ (<http://apps.webofknowledge.com>): Science Citation Index Expanded SCI-EXPANDED from 1945 until now (search performed on July 25, 2012). Each topic search is conveniently accomplished with one or more terms within article titles, abstracts and keywords. Our analysis was intended to give a quantitative impression but is necessarily selective and by no means exhaustive. A reader can easily verify the data, modify our searches and reach his/her own conclusions. Be aware that it does not have a controlled vocabulary (think on synonyms or different ways of expressing the same search).

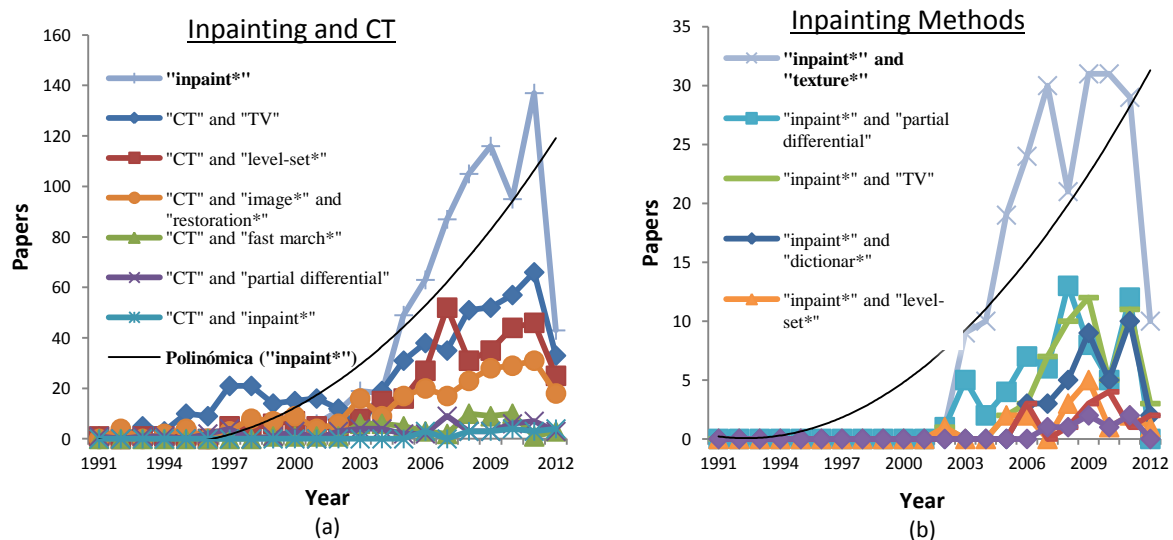





Figure 3-1. Numbers of retrieved papers during 1991–2012 with the searching rules mentioned in each legend (a) Inpainting and CT (b) Inpainting Methods. The polynomial fittings show that there is an 75% increment yearly for the former, while a 70% increment for the latter. Note that the numbers for 2012 are incomplete.

⁴ http://en.wikipedia.org/wiki/ISI_Web_of_Knowledge

  LABORATOIRE D'INTEGRATION DES SYSTEMES ET DES TECHNOLOGIES	Image restoration by inpainting methods applied to CT reconstruction	Réf : DISC/LITT /11 RT000	15
		DATE: 04 09 2012	49
DISC/LITT	Marcos VARGAS	 Révision	1

3.2. 2D Digital Inpainting Software

CImg Library

Download: [CImgLibrary](#) is a C++ template image processing library. Its documentation contains a detailed description of all classes and functions of its library. It has been registered to the APP (French Agency for the Protection of Programs) by the INRIA.

3.3. Metal Artifact Reduction (MAR)

The polynomial fitting in Figure 3-2 shows an 79% increment in the research of “MAR” and “CT”. MAR techniques consists in: (1) using filters, (2) identification and removal of zones by interpolation, (3) directly correction in the retroprojection algorithm, (4) inpainting, our concern.

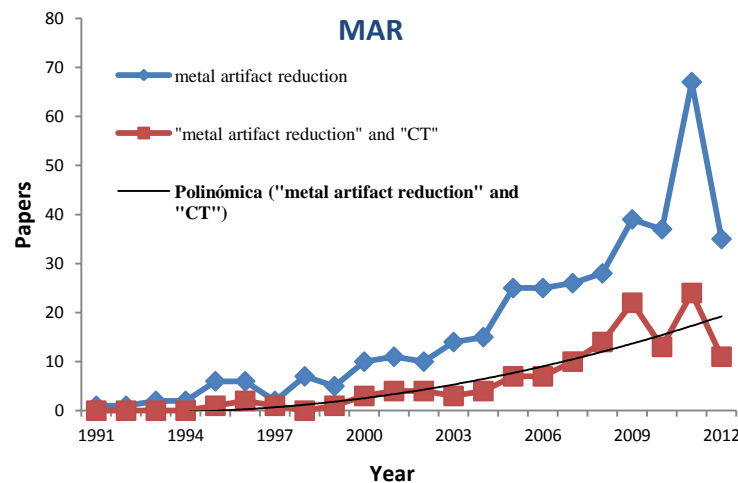





Figure 3-2. (a) MAR SOTA. Flaw charts of some iterative CT algorithms from (b) Y. Li et al. [4] (c)E. Meyer et al. [5]

3.4. Conclusion on our SOTA

Our quantitative literature analyses demonstrated that the scientific publication on “Inpainting and CT” and MAR topics has increased over the last 10 years. This well position our topic in a global research community. This motivate us to research in this topic.

  LABORATOIRE D'INTEGRATION DES SYSTEMES ET DES TECHNOLOGIES	Image restoration by inpainting methods applied to CT reconstruction	Réf : DISC/LITT /11 RT000	16
		DATE: 04 09 2012	49
DISC/LITT	Marcos VARGAS	 Révision	1

Chapter 4

Methods

General Classification

First, we founded a number of already implemented methods. Many of them were developed in C++ or Matlab. Among their application domain, we founded that they are used for: old paintings restoration (filling cracks), artistic purpose, etc. Then, we made a sum up classification on the most representative inpainting families, based-on our SOTA.

2D digital inpainting approaches:

1. PDE methods (non-texture or low-texture images):
 - I: Local/ Transport-type equation [FMM]
 - II: Mimicking the visual system / Denoising viewpoint [TV]
 - III: Anisotropic diffusion that preserves curvature [Tschumperle 05 (inspired on Bertalmio 00)]
 2. Exemplar-based (textures images): From *texture synthesis*⁵ to restoration
 3. Dictionary-based:
 - Elad 05: use implicit texture/decomposition with suitable dictionaries (DCT, Curvelets⁶).
-
-




Figure 4-1. General Classification of Methods in 2D Digital Inpainting.

4.1. Fast Marching Method (FMM) [6]

FMM inpaints the unknown pixels p as a function of all points q in a known neighborhood $B_\epsilon(p)$ by summing the estimates of all points q , weighted by a normalized weighting function $w(p, q)$, as depicted in Figure 4-2.

⁵ http://en.wikipedia.org/wiki/Texture_synthesis

⁶ A higher dimensional generalization of Wavelets, designed to represent images at different scales and angles.

  LABORATOIRE D'INTEGRATION DES SYSTEMES ET DES TECHNOLOGIES	Image restoration by inpainting methods applied to CT reconstruction	Réf : DISC/LITT /11 RT000	17
		DATE: 04 09 2012	49
DISC/LITT	Marcos VARGAS	 Révision	1

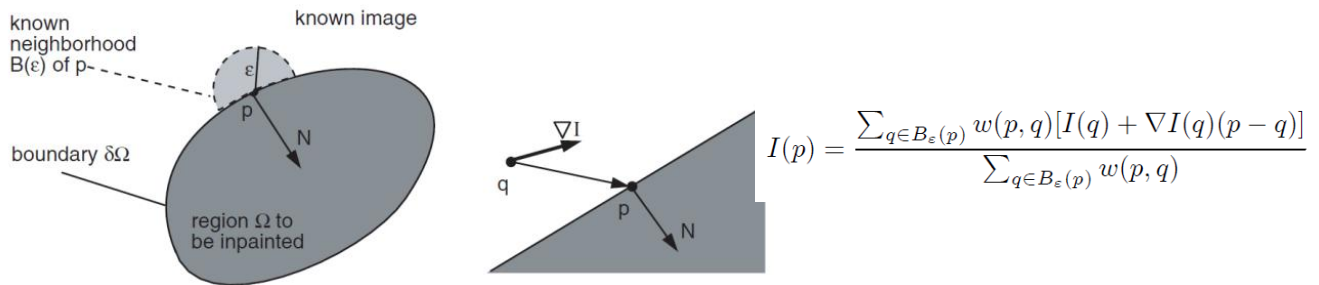


Figure 4-2. FMM: (a) the gray part is the zone to inpaint[6], (b) zoom for gradient in the border[6], (c) equation [6].

Landscape shared in framing, illuminating, and solving problems by 2 computational techniques: **Fast Marching Methods (FMMs)** and **Level Set Methods (LSMs)**. They exploit a fundamental shift in how one views moving boundaries: Eulerian⁷ geometric perspective - PDE⁸; classifying them under *Value Problem (VP)* as [7]:

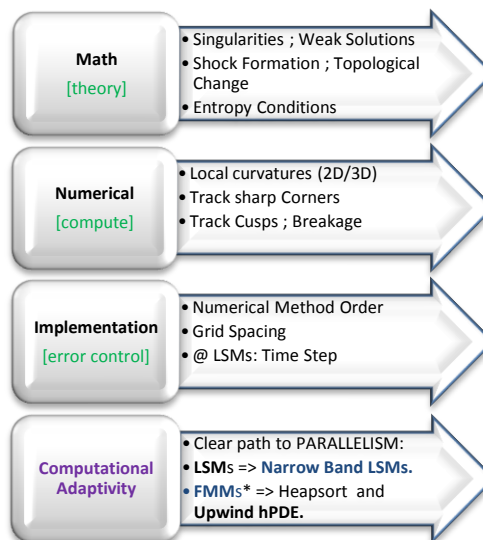


Figure 4-3. FMM Context (*FMMs: Optimal way to solve Hamilton-Jacobi Equation.)

Curvature⁹ \mathbf{k} points in the direction normal to the **Curve**, abuse notation: $F = -\mathbf{k}$

Restrictions:

- 1.- Only \mathbf{eI}^{10} @ Normal direction.
- 2.- F depends only on the local \mathbf{k} : $F = F(\mathbf{k})$

Challenge:

- (1) Accurate scheme for \mathbf{eI} based on (2) [By formulation this \mathbf{eI} @ Eulerian Framework]
- (2) Produce an adequate model for $F = F(\text{Local}; \text{Global}; \text{Indep.})$.

“**FMMs** can be extremely computational efficient, far eclipsing **LSMs**”¹¹ [7]




7 Eulerian Framework : Fixed Coordinate System.

8 PDE = Partial Differential Equation.

9 <http://en.wikipedia.org/wiki/Curvature>

10 Different synonyms for: 'evolving Interface' (eI)= evolving Boundary = evolving Front = moving Interface = Interface Propagation = Interface Motion = Front Motion.

11 For which we have Similarities & Differences (More Details on Appendix 3)

  LABORATOIRE D'INTEGRATION DES SYSTEMES ET DES TECHNOLOGIES	Image restoration by inpainting methods applied to CT reconstruction	Réf : DISC/LITT /11 RT000	18
		DATE: 04 09 2012	49
DISC/LITT	Marcos VARGAS	 Révision	1

4.2. Total Variation (TV)

Figure 4-4 describes the main common definition for TV inpainting methods, where the zone to get inpainted is considered as noisy. Some restoration methods were showed as combining PDE with isotropic, anisotropic diffusion¹² and shock filters¹³, resulting in unified variation approaches [8].

$$v = P u + n$$

P = Linear transformation
 u = Original Image
 v = Noisy Image

n = Additive White Gaussian Noise (AWGN),
 indeed $n \sim N(0, \sigma^2)$

The *inverse problem* can be addressed as to find u that minimizes the energy $E(u)$, as:

$$E(u) = \overbrace{E_1(u)}^{\text{fidelity}} + \lambda \overbrace{E_2(u)}^{\text{regularization } f(\text{grad}(u))}$$

Figure 4-4. TV Context.

We described in the following sub-chapters, five algorithms that belongs to this family.

4.2.1. Naïve Rudin [9][10]

Inspired on fluid dynamics observations, i.e. the use of techniques and concepts under the non-linear hyperbolic PDE solutions, $TV(u) := \int_{\Omega} |\nabla u| dx$ plays an important role for shock¹⁴ calculations, useful to restore discontinuities (edges). We mathematically define Figure 4-5 in Equation Eq. 4.1:

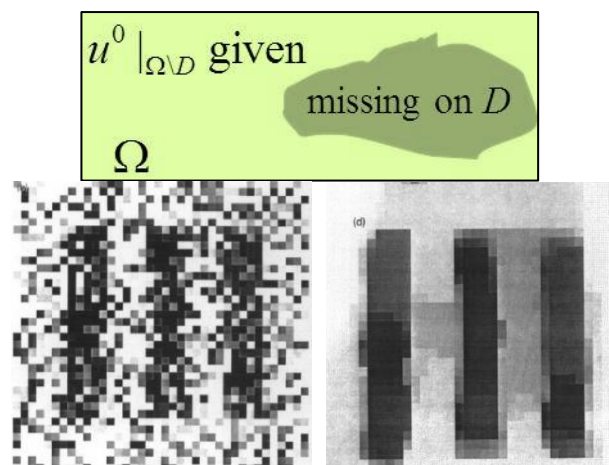





Figure 4-5. (a) Naïve Rudin TV Inpainting model (b) Input [10] (c) Output [10].

¹² Anisotropy is the property of being directionally dependent (also called Perona–Malik diffusion), as opposed to Isotropy, which implies identical properties in all directions. Specifically, Anisotropic Diffusion is a technique aiming at reducing image noise without removing significant parts of the image content, typically edges. It is a non-linear and space-variant transformation of the original image.

¹³ Rudin was the first to introduce the concept of "Shock Filters"

¹⁴ Used for deblurring signals and images. Creates shocks at inflection points

  LABORATOIRE D'INTEGRATION DES SYSTEMES ET DES TECHNOLOGIES	Image restoration by inpainting methods applied to CT reconstruction	Réf : DISC/LITT /11 RT000	19
		DATE: 04 09 2012	49
DISC/LITT	Marcos VARGAS	 Révision	1

Bounded Variation (BV) Regularizer

$$\min_u E[u|u^0, D] = \overbrace{\int_{\Omega} |Du|}^{\text{Bounded Variation (BV) Regularizer}} + \underbrace{\frac{\lambda}{2} \int_{\Omega \setminus D} |Ku - u^0|^2 dx}_{\text{Least Square (for uniform Gaussian Noise)}}$$

Eq. 4.1

The BV norm (Bounded Variation) allows piecewise smooth functions with jumps and is the proper space for this type of discontinuous functions analysis, something well known in the mathematical theory as *shock waves*.

$$\begin{cases} \frac{\partial u}{\partial t} + |\nabla u| F(\nabla u^T H \nabla u) = 0 \\ u(x, y, 0) = u_0(x, y) \end{cases}$$

Figure 4-6 fails to realize the *connectivity principle* of the human disocclusion¹⁵ process.

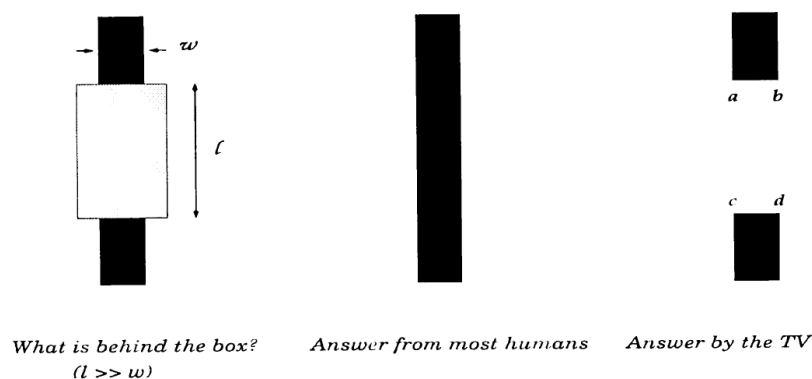





Figure 4-6. Naïve Rudin TV disadvantage [11].

The technique could be interpreted as a first step of moving each level set of the image normal to itself with velocity equal to the curvature of the level set divided by the magnitude of the gradient of the image, and a second step which projects the image back onto the constraint set.

4.2.2. Curvature Driven Diffusion (CDD) [11]

To solve the disadvantage of 4.2.1 Naïve Rudin [10], this method uses a new diffusion mechanism: *the conductivity coefficient* depends on the curvature of the isophotes¹⁶.

¹⁵ Recovery of occluded areas in a digital image
¹⁶ A contour of equal luminance in an image.

  LABORATOIRE D'INTEGRATION DES SYSTEMES ET DES TECHNOLOGIES	Image restoration by inpainting methods applied to CT reconstruction Marcos VARGAS	Réf : DISC/LITT /11 RT000	20
		DATE: 04 09 2012	49
DISC/LITT		 Révision	1

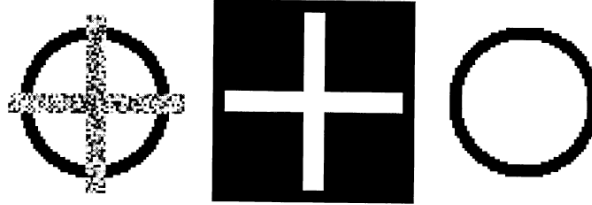


Figure 4-7. CDD: Connectivity Principle (a)Input (b)Mask (c) Output [11] (i.e. using straight lines for circular arcs)

We have a 3rd order divergence form as follows:

$$\begin{cases} \frac{\partial u}{\partial t} \text{ (or } 0) = \nabla \cdot \left[- \left[\frac{g(|k|)}{|\nabla u|} \nabla u \right] \right] = -\nabla \cdot \mathbf{j} & , x \in D \\ u = u^0 \text{ (available part of the image),} & x \in D^c \end{cases}$$

4.2

The explicit scheme iterates as: $u^{(n+1)} = u^n - \Delta t \nabla \cdot \mathbf{j}^n |_{\Delta t = \text{time step}}$

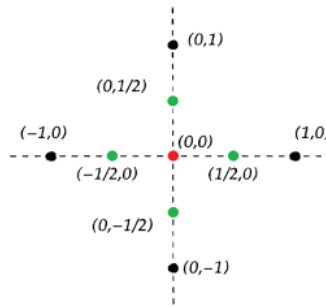


Figure 4-8. Divergence Operator: Grid of a given image, around pixel (0,0) [inspired on [11]]

The divergence form $\nabla \cdot \mathbf{j}$ is discretized, assuming $\mathbf{j} = (\mathbf{j}^1, \mathbf{j}^2)$. We will test for $(\frac{1}{2}, 0)$:

$$\begin{aligned} & \frac{j_{(\frac{1}{2},0)}^1 - j_{(-\frac{1}{2},0)}^1}{h} + \frac{j_{(0,\frac{1}{2})}^2 - j_{(0,-\frac{1}{2})}^2}{h} \\ \nabla u_{(\frac{1}{2},0)} &= \left(\frac{\partial u}{\partial x} \Big|_{(\frac{1}{2},0)}, \frac{\partial u}{\partial y} \Big|_{(\frac{1}{2},0)} \right) \cong \left(\frac{u_{(1,0)} - u_{(0,0)}}{h}, \frac{u_{(\frac{1}{2},1)} - u_{(\frac{1}{2},-1)}}{2h} \right) \end{aligned}$$

$$k = \nabla \cdot \left[\frac{u}{|\nabla u|} \right] = \frac{\partial}{\partial x} \left[\frac{u_x}{|\nabla u|} \right] + \frac{\partial}{\partial y} \left[\frac{u_y}{|\nabla u|} \right] \xrightarrow{\text{yields}} k_{(\frac{1}{2},0)} = \left(\left[\frac{u_x}{|\nabla u|} \right]_{(1,0)} - \left[\frac{u_x}{|\nabla u|} \right]_{(0,0)} \right) + \left(\left[\frac{u_y}{|\nabla u|} \right]_{(1,0)} - \left[\frac{u_y}{|\nabla u|} \right]_{(0,0)} \right)$$

For the pending expressions as $\frac{u_x}{|\nabla u|}$, we just simplify the ordinary pixel wise central difference as Figure 4-8.

4.2.3. Mean Curvature Diffusion (MCD) [12]

This is an approach for introducing ideas from computational fluid dynamics into problems in image analysis. Navier-Stokes equations has the advantage of well-developed theoretical and numerical results. The method uses ideas from classical fluid dynamics (Navier-Stokes equations) to propagate isophote lines continuously from the exterior into the region to be inpainted. The idea is to consider of the image intensity as a 'stream function' for a two-dimensional incompressible flow. The Laplacian of the image intensity plays the role of the vorticity of the fluid [12]; it is transported into the region to be inpainted by a vector field defined by the stream function.

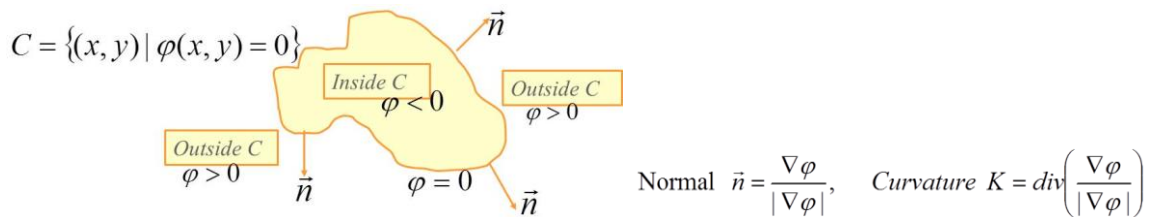


Figure 4-9. MCD, mathematical definition.

C = boundary of an open domain. Originally developed for tracking fluid interfaces, Allows automatic topology changes, cusps, merging and breaking.



Figure 4-10. (a) Comparative table on the implemented ideas [12] (b) Result of the algorithm [12]

4.2.4. Euler's Elastica: CDD and MCD Combined [13]

Euler's Elastica unifies the early works of Chan and Shen [11] on CDD (motivated by human visual perception), and that of Bertalmio, Bertozzi and Sapiro [12] on MCD (transport based inpainting).

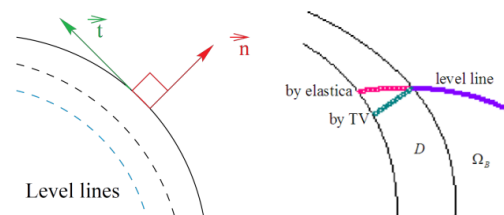





Figure 4-11. (a) Tangent and Normal (b) Euler's Elastica vs TV. [14]

The elastica model [13] minimizing the Euler's Elastica energy is Eq. 4.3. :

  LABORATOIRE D'INTEGRATION DES SYSTEMES ET DES TECHNOLOGIES	Image restoration by inpainting methods applied to CT reconstruction	Réf : DISC/LITT /11 RT000	22
		DATE: 04 09 2012	49
DISC/LITT	Marcos VARGAS	 Révision	1

$$\min_u \left\{ J(u) = \int_{\Omega} (a + b|k|^p) |\nabla u| dx dy + \frac{\lambda}{2} \int_{\Omega \setminus D} (u - z)^2 dx dy \right\}$$

4.3

Where a and b are arbitrary positive constants, $\lambda > 0$ is a penalty parameter, $p = 2$ is usually chosen, $u = u(x, y)$ is the true image to be restored and $k = k(x, y) \equiv \nabla \cdot \frac{\nabla u}{|\nabla u|}$ is the curvature. The virtue of 4.3 is that the regularization using the Euler's Elastica energy penalizes the integral of the square of the curvature along edges instead of only penalizing the length of edges as the TV model (if taking $b = 0$) does [15]. Consequently the model can reconnect contours along large distances and recover the curvature of objects at the same time.

For its numerical implementation, we used the notation displayed in Figure 4-12.

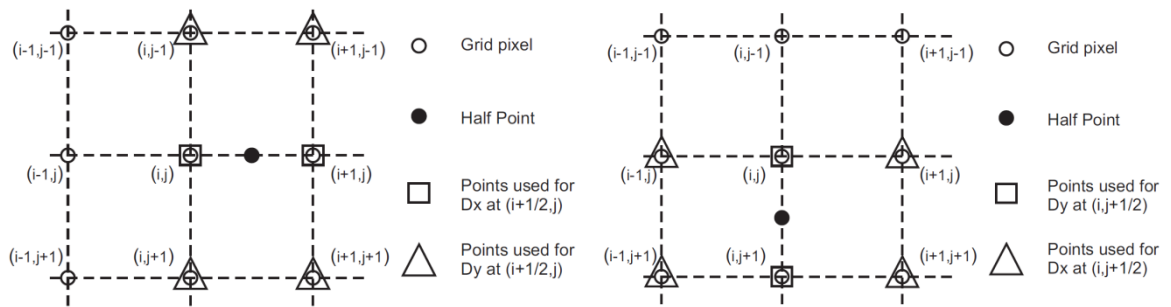


Figure 4-12. On the left side an x-half-point and on the right side a y-half-point [15].

Doing a review of numerical methods for its solution, we found (a) An accelerated time marching method [ATM]; and (b) *Texture-synthesis*-based algorithm. They have in common the use of central differences between ghost half-points, see Figure 4-12.

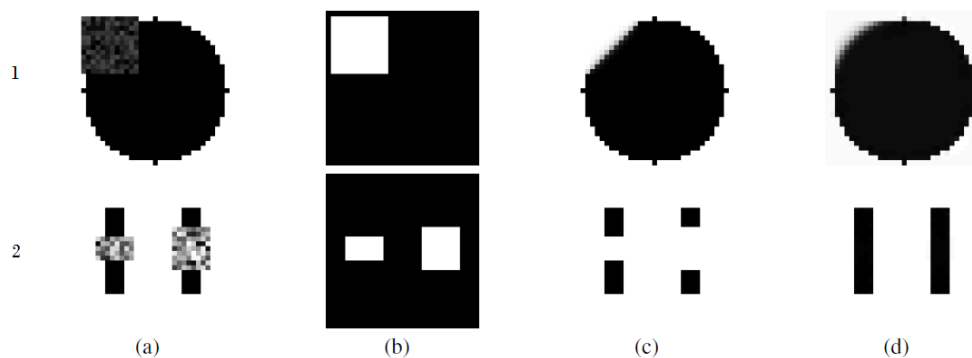





Figure 4-13. Naïve Rudin vs Euler's Elastica. Rows (1): Circle problem, (2): Broken bars problem. Columns (a) Images with different sizes for the occluding noisy squares, (b) mask, (c) Rudin result, (d) Euler's Elastica result. [15]

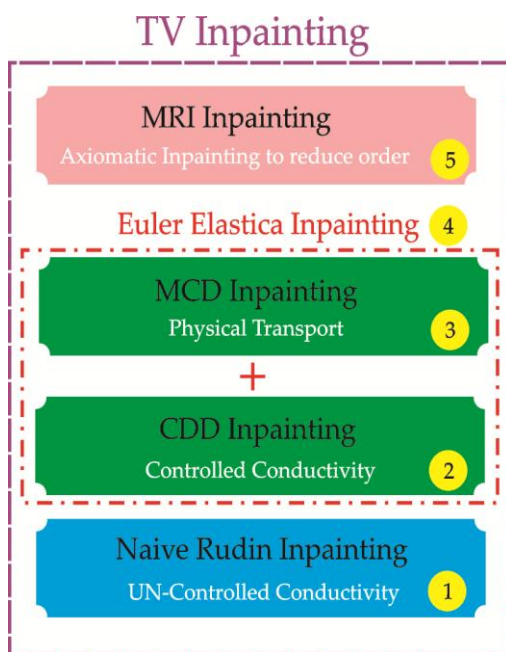
  LABORATOIRE D'INTEGRATION DES SYSTEMES ET DES TECHNOLOGIES	Image restoration by inpainting methods applied to CT reconstruction	Réf : DISC/LITT /11 RT000	23
		DATE: 04 09 2012	49
DISC/LITT	Marcos VARGAS	 Révision	1

4.2.5. Morphologically Rotation Invariant (MRI) [16]

The contribution of MRI is an *Axiomatic Inpainting* to reduce the model from 4th [13] to 3th order, so that it is more stable and faster than MCD.

4.2.6. Conclusion on TV Inpainting Families

We have studied TV models that are closely connected to the classical TV denoising model of Rudin, for inpaintings involving the recovery of edges. The BV Regularizer is Insufficient for Inpainting. Curvature processing imposes in cooperation theoretical & computational challenges (nonlinear 3rd and 4th order PDEs), having cognitive/perceptual foundation.



- 1) **Naïve Rudin Inpainting:** uses a naïve Rudin/Osher/Fatemi model. It works but the bad control of the conductivity factor, does not permit to use this filter on medium size inpainting areas. The TV inpainting is very similar to Oliveira inpainting.
- 2) **CDD Inpainting:** is a TV inpainting with controlled conductivity on the basis of the local curvature. This is a useful information to enhance Oliveira inpainting.
- 3) **MCD Inpainting:** is a physical transport inpainting. It is complementary of the CDD inpainting.
- 4) **Euler's Elastica Inpainting:** Combines MCD and CDD inpaintings together for having both properties.
- 5) **MRI Inpainting:** Reduce the model from 4th to 3th order.

Figure 4-14. TV Inpainting Family



4.3. Anisotropic Diffusion-Based (AdB) [17]

Tschumperle proposes in [17] an efficient second-order anisotropic diffusion model for multi-valued image regularization and inpainting. The pixels in this inpainting domain are iteratively updated according with a finite difference approximation to the equations $\frac{\partial u_i}{\partial t} = \text{trace}(T \nabla^2 u_i)|_{i \in \{1 \dots N\}}$. Here,

$$T \text{ is the tensor field defined as: } T = \frac{1}{(1+\lambda_{min}+\lambda_{max})^{\alpha_1}} v_{min} \otimes v_{min} + \frac{1}{(1+\lambda_{min}+\lambda_{max})^{\alpha_2}} v_{max} \otimes v_{max} ,$$

With $0 < \alpha_1 \ll \alpha_2$, and $\lambda_{min}, \lambda_{max}, v_{min}(\vec{V}_1), v_{max}(\vec{V}_2)$ are the eigenvalues and eigenvectors,

respectively of \widehat{G}_σ * $\sum_{i=1}^N \nabla u_i \otimes \nabla u_i$. The classical structure tensor is known for representing well the local geometry of the image (Figure 4-15.)

 list LABORATOIRE D'INTEGRATION DES SYSTEMES ET DES TECHNOLOGIES	Image restoration by inpainting methods applied to CT reconstruction	Réf : DISC/LITT /11 RT000	24
		DATE: 04 09 2012	49
DISC/LITT	Marcos VARGAS	 Révision	1

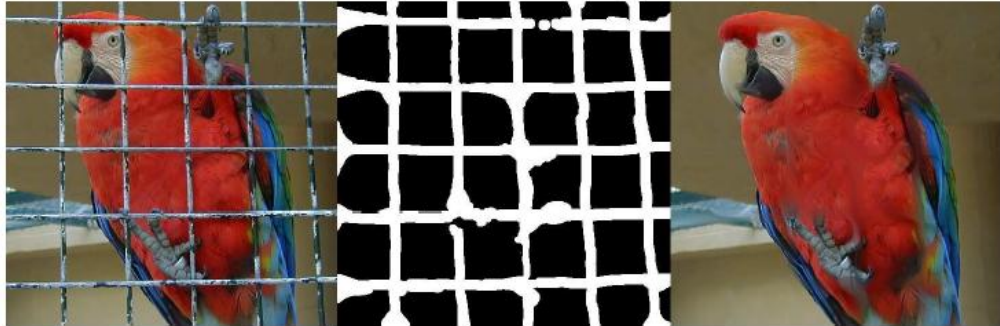


Figure 4-15. AdB inpainting technique, where the image in the center is the mask defined by the user[17].

This anisotropic diffusion that preserves curvature comes from the idea of the diffusion equation

$\frac{\partial I_{[x,y;t]}}{\partial t} = \text{div}(c[x,y;t] \times \nabla I[x,y;t])$. Based on that idea, Tschumperle's proposition is:

$$\frac{\partial I_i}{\partial t} = \text{trace}([C_1 \vec{V}_1 \vec{V}_1^T + C_2 \vec{V}_2 \vec{V}_2^T] H_i) \Big|_{v_i=1\dots n} \quad 4.4$$

n = Vector Dimension of the Image I , if $n = 3$ then (R,G,B).

C_1, C_2 = Positive weights. \vec{V}_1, \vec{V}_2 = Eigenvectors. I, O = input, output and α = regularization factor.

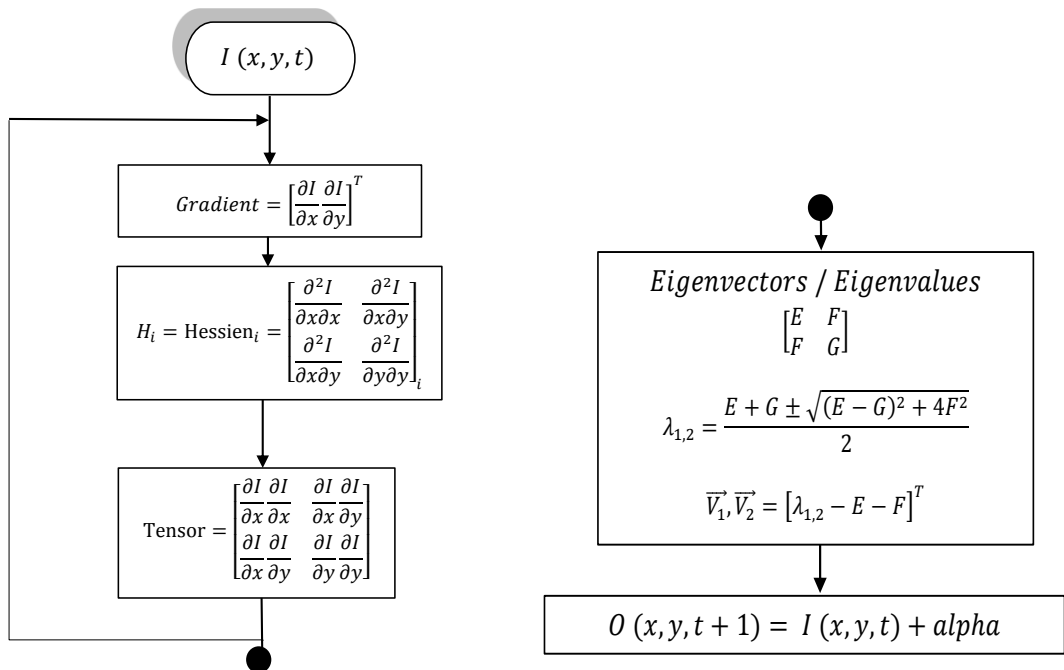




Figure 4-16. Flow Diagram of the AdB algorithm.

 list LABORATOIRE D'INTEGRATION DES SYSTEMES ET DES TECHNOLOGIES	Image restoration by inpainting methods applied to CT reconstruction	Réf : DISC/LITT /11 RT000	25
		DATE: 04 09 2012	49
DISC/LITT	Marcos VARGAS	 Révision	1

4.4. Exemplar-Based (ExB) [18]

The exemplar based methods fill the missing areas with copies of neighboring areas which match certain criteria. The algorithms search patches in the known neighborhood (the user could change their size as for example 3x3 pixels, etc), for which priority coefficients are computed. The algorithm described in [18] maximizes the priority and hence the corresponding patch (exemplar) that is copied to the missing area (area to inpaint). In order to comprehend the region filling process, all the concepts are color described in colors in Figure 4-17. Given the patch ψ_p (green rectangle, centered at point p), \mathbf{n}_p is the normal to the contour $\partial\Omega$ (front) of the target region Ω (zone to inpaint, i.e. to be removed and filled, white part) and ∇I_p^\perp is the isophote (in blue, direction and intensity) at point p . The entire image is denoted with I . From the previous definitions, we can infer that:

$\phi = (I - \Omega)$, is the source region. Also $\Omega + \bar{\Omega} = I$. $\mathbf{n}_p =$ unit vector orthogonal to $\partial\Omega$ at point p .

Point $p \in \partial\Omega$. $|\psi_p| =$ area of ψ_p .

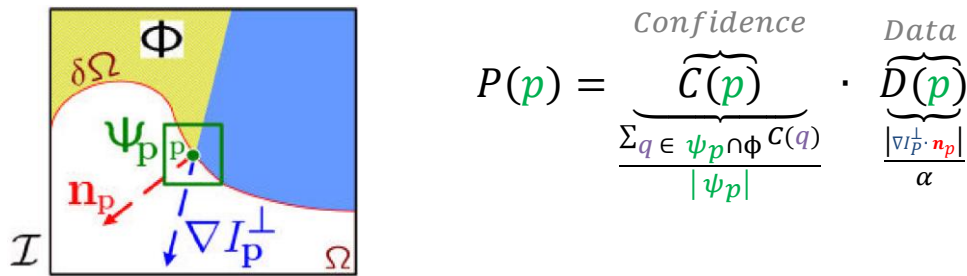


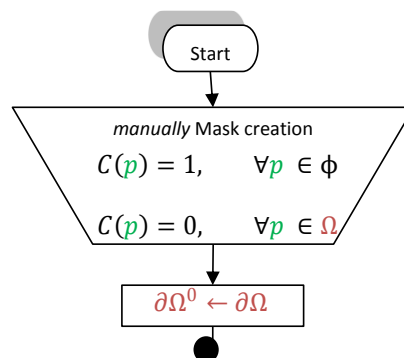
Figure 4-17. (a) ExB Basic Diagram [18] (b) ExB formula.

where α is a normalization factor (e.g. $\alpha = 255$ for a typical grey-level image).

The distance $d(\psi_{\hat{p}}, \psi_{\hat{q}})$ between two patches is defined as the sum of squares differences (SSD) of the already filled pixels in the two patches.

$$\text{Update } C(p) = C(\hat{p}), \forall p - p \in \psi_{\hat{p}} \cap \Omega$$

Pixels along the fill front ($\partial\Omega$) receive temporarily a priority value in order to determine the order of filling. The algorithm iterates in three main steps described in Figure 4-18, until all pixels are filled. “This simple update rule allows us to measure the relative confidence of patches on the fill front, without image specific parameters. As filling proceeds, confidence values decay, indicating that we are less sure of the color values of pixels near the center of the target region.” [18].



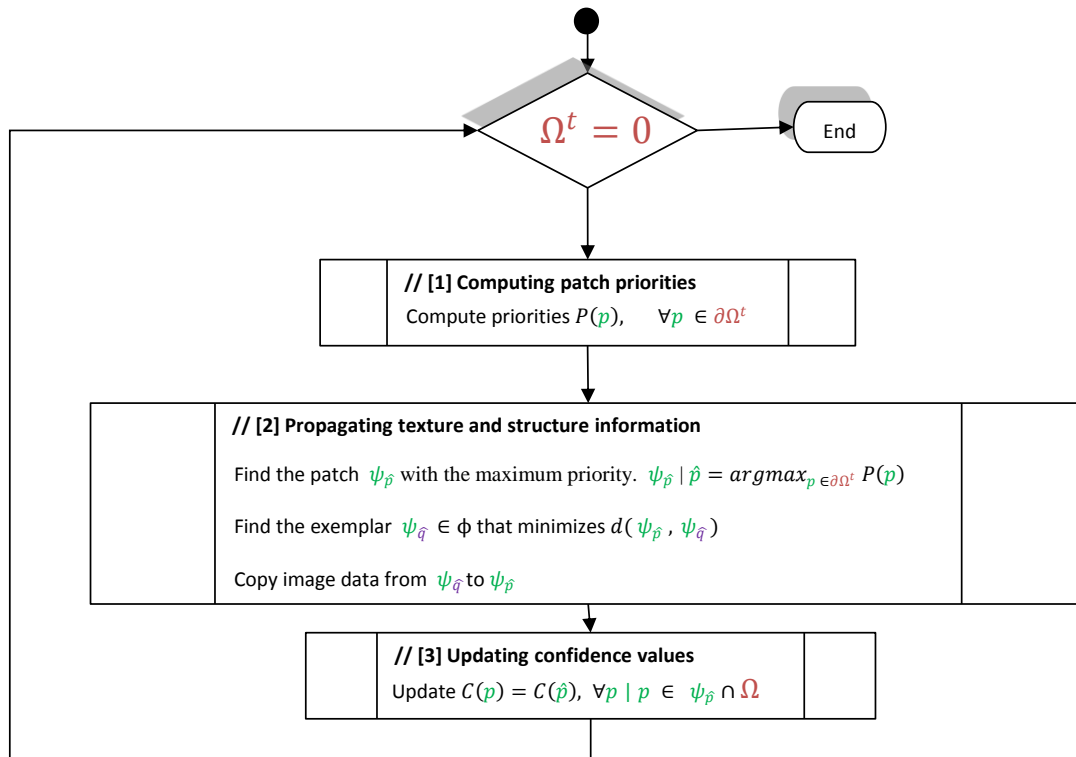


Figure 4-18. Flow Diagram of the ExB algorithm.

4.5. Conclusion

Even though we have seen that there are a large variety of image restoration methods which offer many advantages, we have also become aware of some limitations. Figure 4-19 gives an overview on all the inpainting methods discussed in this chapter. It became clear in 4.4 Exemplar-Based (ExB) that the image's patches provide a good *dictionary* to complete other parts of the image. Finally, the UML diagrams of some of the most representative methods are available in the Appendix 3.

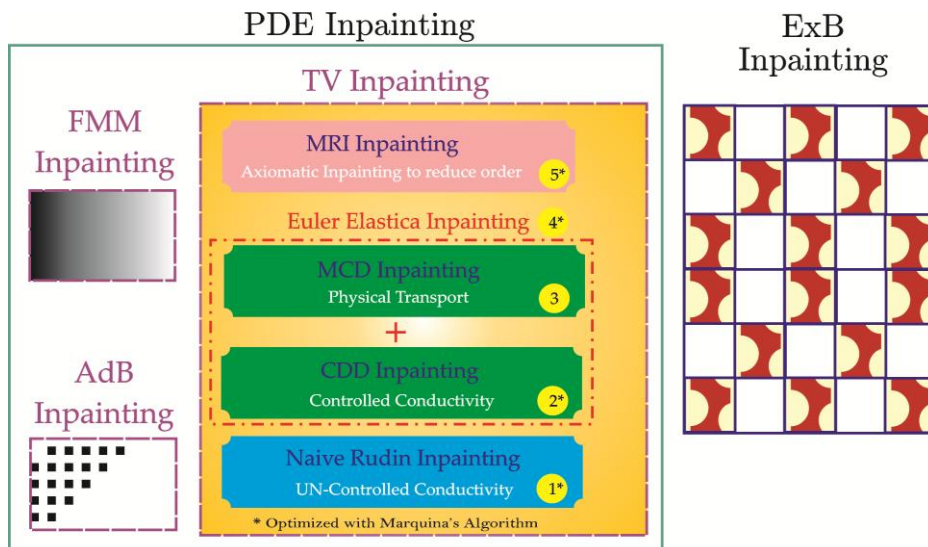




Figure 4-19. Our general 2D digital inpainting methods classification.

 list LABORATOIRE D'INTEGRATION DES SYSTEMES ET DES TECHNOLOGIES	Image restoration by inpainting methods applied to CT reconstruction	Réf : DISC/LITT /11 RT000	27
		DATE: 04 09 2012	49
DISC/LITT	Marcos VARGAS	 Révision	1

Chapter 5

Results and Discussion

This chapter presents the most illustrative results obtained during our work. We focus on the evaluation and validation of the eight inpainting algorithms proposed, under the projection and sinogram domain. Following the usual validation procedure, we describe first the results obtained from simple synthetic images, then the realistic synthetic images and finally the results from real images.

5.1. Materials

5.1.1. PC and IDE

All algorithms were tested in a normal user PC, a Lenovo ThinkStation, with a processor Intel Xeon @ 2.53 GHz (6 GB RAM). The IDE was Microsoft Visual Studio 2010 Professional, running under Windows 7 Enterprise 64bits (SP1).

5.1.2. Simple Synthetic Images using Paint®

We needed simple geometric forms to start testing the inpainting techniques, as in Figure 5-1.

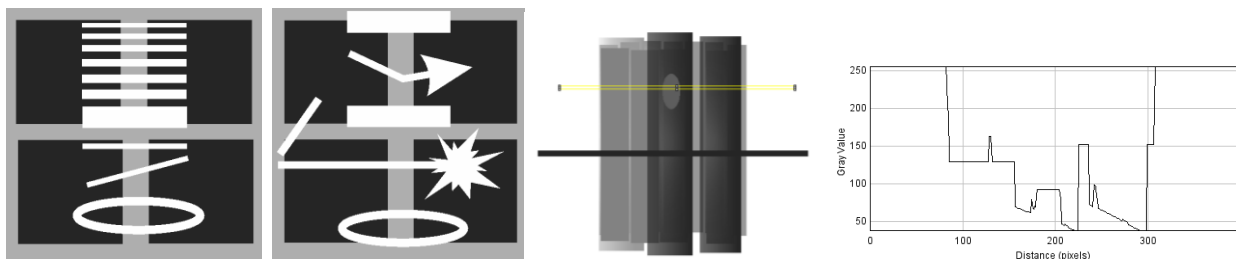





Figure 5-1. (a)(b)(c) Simple geometric forms; (d) 24-bit Bitmap profile of c (simple version of Figure 5-2).

5.1.3. Simulated Images using CIVA®

The x-ray simulation software CIVA has been developed to help the design stage of radiographic systems, to enable performance demonstration and to optimize the testing process [19]. In this context, we use its CT module for our case under CIVA platform (Figure 5-2).

  LABORATOIRE D'INTEGRATION DES SYSTEMES ET DES TECHNOLOGIES	Image restoration by inpainting methods applied to CT reconstruction	Réf : DISC/LITT /11 RT000	28
		DATE: 04 09 2012	49
DISC/LITT	Marcos VARGAS	 Révision	1

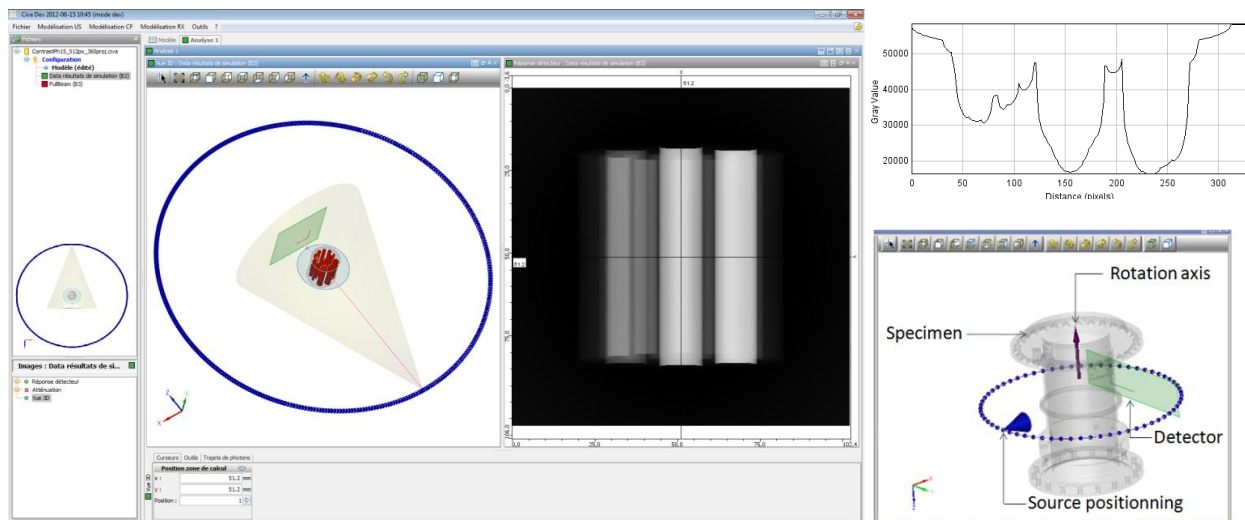


Figure 5-2. CIVA, (a) scene and CT setup, (b) 16-bit TIFF profile, (c) tomography displacement [19].

5.1.4. Experimental Images using SkyScan2011®

The SkyScan2011 x-ray nanotomograph is a revolutionary laboratory nano-CT scanner with spatial resolution in the range of hundreds of nanometers. This spatial resolution in volume terms is equal to or better than that of synchrotron tomography. The 2011 nano-CT employs an open-type x-ray source with a LaB_6 cathode with a focal spot size of less than 400nm. At this small spot size, small-angle scattering enhances object details down to 150-200nm. A sophisticated object manipulator allows object positioning and rotation with an accuracy of better than 100nm. The x-ray detector is based on an intensified CCD with single photon sensitivity. The object is scanned under normal environmental conditions, without any coating, vacuum treatment or other preparation. [These details were taken from <http://www.skyscan.be/products/2011.htm>] In our case, Figure 5-3 (c) was chosen to obtain a pixel size of 1.2 μm and we acquired 360 projections of 1280 \times 1024 pixels.

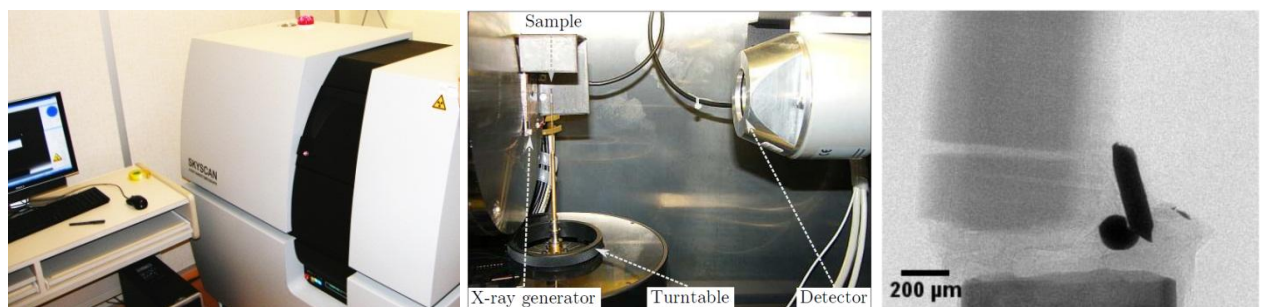





Figure 5-3. The Nano-CT device SkyScan2011:(a) External view, (b)Internal view[20],(c) Projection image @ 0° [20].

5.1.5. Experimental Images using PerkinElmer®

In our laboratory a 40 cm by 40 cm flat-panel detector is used for radiographic and tomographic inspection of large objects. It is an array of 2048 x 2048 pixels of 200 microns and its main advantages are the fast acquisition and the high efficiency for a large energy interval. [These details were taken from <http://www.perkinelmer.com/fr/pages/020/imaging/micro-ct-technology.xhtml>].

  LABORATOIRE D'INTEGRATION DES SYSTEMES ET DES TECHNOLOGIES	Image restoration by inpainting methods applied to CT reconstruction	Réf : DISC/LITT /11 RT000	29
		DATE: 04 09 2012	49
DISC/LITT	Marcos VARGAS	 Révision	1

A picture of the experimental setup is displayed in Figure 5-4 together with the imaged sample and a radiographic image.

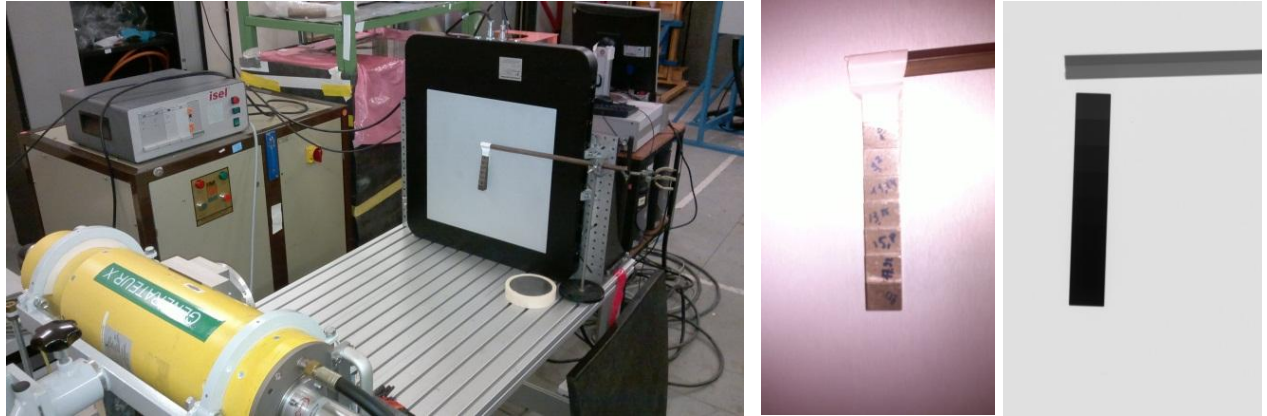


Figure 5-4. PerkinElmer device:(a) external view (b) material position (c) projection image @ 0°.

5.2. Methodology

Our 3-step planning (Figure 5-5), started by the inpainting algorithms evaluation in three types of images, ordered by complexity. (1) Simple Synthetics Images, useful material for the initial coding steps. With that experience, we moved on a little more complex images: (2) Realistic Synthetic Images, simulated by CIVIA. Finally, we applied the algorithms on (3) Real Images, experimental images generated by SkySCAN and PerkinElmer.

PLANNING




1. **Evaluation of Inpainting Algorithms**
 - Simple Synthetic Images: Simple geometric forms (Paint)
 - Realistic Synthetic Images: X-ray attenuation simulated images (CIVA)
 - Real Images: Experimental images (SkySCAN, PerkinElmer)

→ Image Quality Assessment: Choice of the adapted algorithm
2. **Algorithm Optimization and Test on Sinograms**
 - Optimization for fast inpainting execution
 - Semi-automatic mask creation
3. **Validation on CT images**
 - Noiseless and noisy images

Figure 5-5. Our 3-step planning, an insight on our evaluation techniques.

5.2.1. Mask

The mask can be seen as a binary image that tells to the algorithm where is the known information and the unknown. So that, the information will be taken from the known parts to fill in the unknown parts. It is an intrinsic definition of inpainting. Their internal form will have a direct impact of the final results. Mask has to be of the same size of the image to inpaint.

  LABORATOIRE D'INTEGRATION DES SYSTEMES ET DES TECHNOLOGIES	Image restoration by inpainting methods applied to CT reconstruction	Réf : DISC/LITT /11 RT000	30
		DATE: 04 09 2012	49
DISC/LITT	Marcos VARGAS	 Révision	1

5.2.2. Image Quality Assessment

For a proper assessment of the results, only a visual comparison is not sufficient since it may be subjective. Therefore in order to perform a quantitative evaluation we use several image quality indicators. The first which is also the simplest and most widely used, is the mean squared error (MSE). The second is the peak signal-to-noise ratio (PSNR). The third is the Multi-Scale Structural Similarity Index (MS-SSIM Index). It is used because it is based on the structural information degradation (human visual perception is highly adapted for extracting structural information from a scene). MS-SSIM compares local patterns of pixel intensities that have been normalized for *luminance* and *contrast* [20].

Summing-up, we used: MSE ($\blacksquare = 0$), PSNR ($\blacksquare = \infty$) and MS-SSIM ($\blacksquare = 1$).

\blacksquare = Ideal case, when an image inpainted is equal to the original.

5.3. Evaluation on:

5.3.1. Simple Synthetic Images

Our SOTA (Chapter 3), helped us only to consider the main family methods. As, there are different algorithms inside each family, we made a pre-selection step by testing other options with this simple geometric forms. After that, we decided to use only the algorithms previously describe in Chapter 4. They are eight inpainting techniques (summarized in Figure 4-19): FMM (4.1), TV Rudin (4.2.1), CDD (4.2.2), MCD (4.2.3), Euler's Elastica (4.2.4), MRI (4.2.5), AdB (4.3) and ExB (4.4).

We started this work by testing the inpainting techniques chosen, using the simple synthetic images created (Figure 5-6).

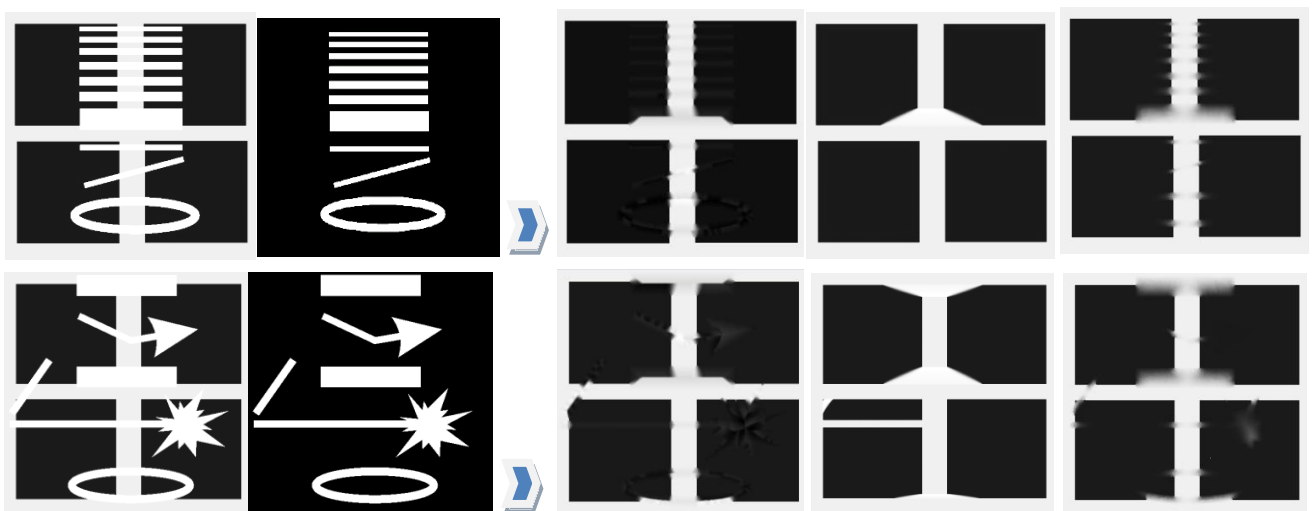


Figure 5-6. Simple Synthetic images (509 x 506 px.) created for initial tests: (a) image with white parts representing lost information, (b) mask, (c) FMM, 25s. 50k iterations. (d) AdB, 62517.4 s. 60.3k iterations (e) CDD, 76.45 s.

It becomes evident from Figure 5-6, that the AdB inpainting (Tschumperle's algorithm) gives the best result, regardless time. Even if the AdB inpainting gave the best result in this simple synthetic images, AdB will not give any advantages for our cases in real images (as it will be seen after).

A synopsis (Figure 5-7), on how our approach will help for a CT reconstruction. The first step inpaints in the Projection domain (red [1P]), the second one inpaints in the Sinogram domain (blue [2S]), and the third one compares the previous results and looks for image quality metrics (orange [3Q]). Note that in Figure 5-7, ν is a ramp filter (before the back projection is performed).

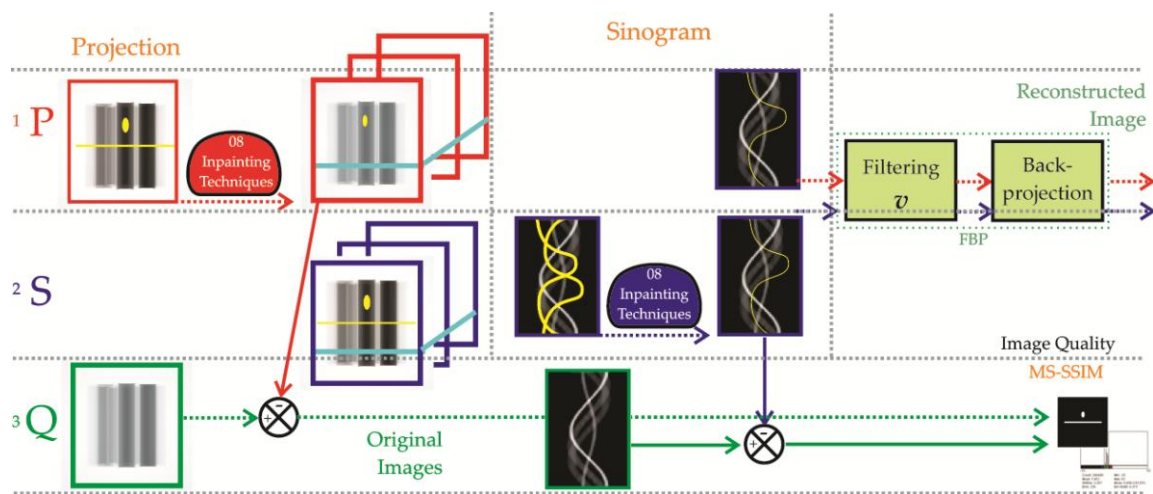


Figure 5-7. Overview of the 2 different domains: Projection and Sinogram.

5.3.2. A CT Realistic Synthetic Image from CIVA (noiseless) in Projection

Lines and circles symbolize real artifact in size and form (Figure 5-8), as well as small defects in the sensor. Different masks were created. In all the mask, the white part represent the zone where the inpainting will be done. The zones to inpaint are less than 6 % of the total image. The original images format is 16-bit TIFF. They are exported as 24-bit Bitmap to perform each inpainting process. Figure 5-8 helps to understand the different positions on the coming Figures.



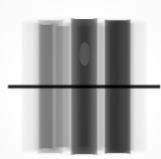

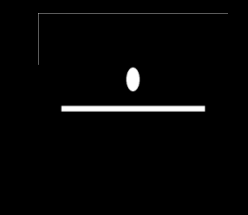


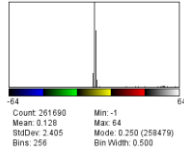

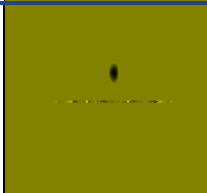
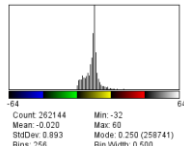


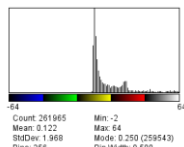


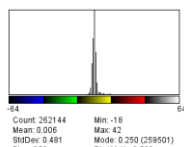


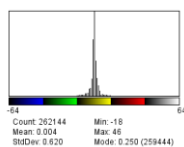
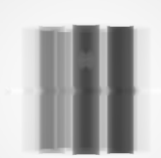

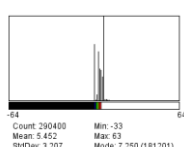

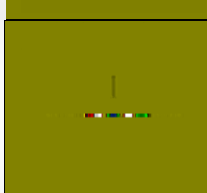
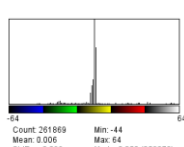


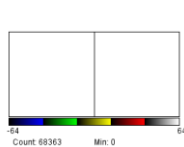



original image (OI)	Image with Artifact (IwA)	calibration bar 	Mask	image source dimension
inpainting method name (M)	result after inpainting with M the IwA (R)	(OI - R) lookup table 5-ramps (BKG value =0.0)	histogram of (OI - R)	processing time 3 image quality metrics
Inpainting Method	Final Results	Comparative Fig.	Histogram	Image Quality

Figure 5-8. Legend for the next results.

	 			Source: CIVA 512 x 512 px.
TV Rudin			 <p> Count: 261690 Min: -1 Mean: 0.128 Max: 64 StdDev: 2.405 Mode: 0.250 (258479) Bins: 256 Bin Width: 0.500 </p>	3.55 s. MSE: 29 PSNR: 33.46 dB MS-SSIM: 0.8291
Curvature Driven Diffusion (CDD)			 <p> Count: 262144 Min: -32 Mean: -0.020 Max: 60 StdDev: 0.993 Mode: 0.250 (258741) Bins: 256 Bin Width: 0.500 </p>	9.83 s. MSE: 0.9 PSNR: 48.61 dB MS-SSIM: 0.8439
MCD			 <p> Count: 261965 Min: -2 Mean: 0.122 Max: 60 StdDev: 1.968 Mode: 0.250 (258543) Bins: 256 Bin Width: 0.500 </p>	618.10 s. MSE: 10 PSNR: 38.27 dB MS-SSIM: 0.8391
Euler's Elastica			 <p> Count: 262144 Min: -18 Mean: 0.006 Max: 42 StdDev: 0.491 Mode: 0.250 (258501) Bins: 256 Bin Width: 0.500 </p>	19.47 s. MSE: 0.3 PSNR: 52.96 dB MS-SSIM: 0.8431
MRI			 <p> Count: 262144 Min: -18 Mean: 0.004 Max: 46 StdDev: 0.820 Mode: 0.250 (258444) Bins: 256 Bin Width: 0.500 </p>	5.35 s. MSE: 0.5 PSNR: 51.29 dB MS-SSIM: 0.8401
FMM			 <p> Count: 290400 Min: -33 Mean: 5.452 Max: 63 StdDev: 3.207 Mode: 0.250 (191201) Bins: 256 Bin Width: 0.500 </p>	13.13 s. MSE: 39 PSNR: 26.76 dB MS-SSIM: 0.7380
AdB (stopped at 13.3 k iterations)			 <p> Count: 261669 Min: -44 Mean: 0.006 Max: 64 StdDev: 2.299 Mode: 0.250 (258376) Bins: 256 Bin Width: 0.500 </p>	10534.68 s. MSE: 25 PSNR: 34.16 dB MS-SSIM: 0.8043
Exemplar Based (ExB) patch size: 4 x 4 px.			 <p> Count: 68363 Min: 0 Mean: 0 Max: 0 StdDev: 0 Mode: 0.250 (68363) Bins: 256 Bin Width: 0.500 </p>	42.12 s. MSE: 0.1 PSNR: 57.81 dB MS-SSIM: 0.9899

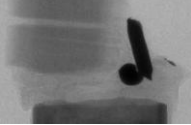
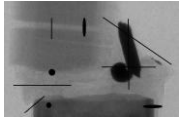

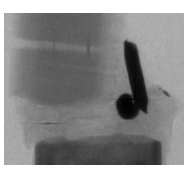

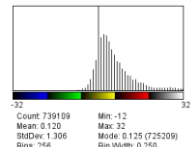
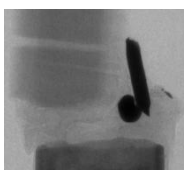

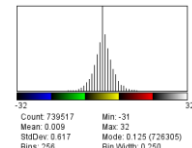
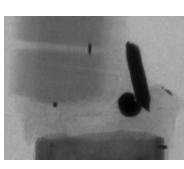
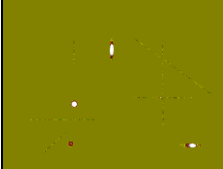
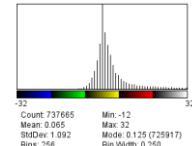
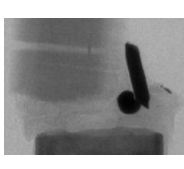
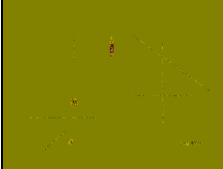
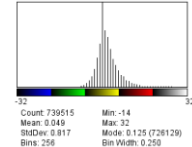
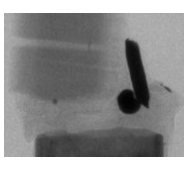
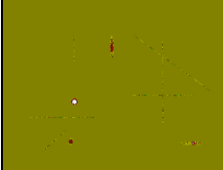
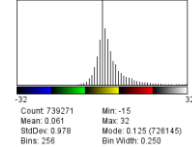
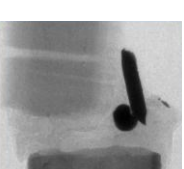

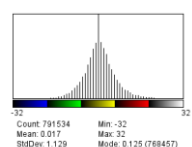
  LABORATOIRE D'INTEGRATION DES SYSTEMES ET DES TECHNOLOGIES	Image restoration by inpainting methods applied to CT reconstruction	Réf : DISC/LITT /11 RT000	33
		DATE: 04 09 2012	49
DISC/LITT	Marcos VARGAS	 Révision	1




Inpainting Method	Final Result	Comparative Fig.	Histogram	Image Quality
-------------------	--------------	------------------	-----------	---------------

Figure 5-9. Test on Noiseless Images (CIVA). Internal images were cropped to 103 x 103 for visibility.

The best four results were highlighted with blue, and they are: CDD, Euler's Elastica, MRI, and ExB.

5.3.3. CT Real Images from SkyScan2011 and PerkinElmer (noisy) in Projection.

				Source: SkyScan2011 1061 x 697 px.
				
TV Rudin			 Count: 739109 Min: -12 Mean: 0.120 Max: 32 StdDev: 1.206 Mode: 0.125 (726309) Bins: 256 Bin Width: 0.250	12.65 s. MSE: 2.7 PSNR: 41.32 dB MS-SSIM: 0.8983
Curvature Driven Diffusion (CDD)			 Count: 739517 Min: -31 Mean: 0.009 Max: 32 StdDev: 0.817 Mode: 0.125 (726305) Bins: 256 Bin Width: 0.250	34.14 s. MSE: 0.2 PSNR: 52.98 dB MS-SSIM: 0.9232
MCD			 Count: 737665 Min: -12 Mean: 0.065 Max: 32 StdDev: 1.092 Mode: 0.125 (726117) Bins: 256 Bin Width: 0.250	117.78 s. MSE: 8.4 PSNR: 36.42 dB MS-SSIM: 0.9006
Euler's Elastica			 Count: 730515 Min: -14 Mean: 0.049 Max: 32 StdDev: 0.817 Mode: 0.125 (726129) Bins: 256 Bin Width: 0.250	69.74 s. MSE: 0.6 PSNR: 48.17 dB MS-SSIM: 0.9185
MRI			 Count: 739271 Min: -15 Mean: 0.061 Max: 32 StdDev: 0.978 Mode: 0.125 (726145) Bins: 256 Bin Width: 0.250	19.13 s. MSE: 1.3 PSNR: 44.75 dB MS-SSIM: 0.9191
FMM			 Count: 791534 Min: -32 Mean: 0.017 Max: 32 StdDev: 1.129 Mode: 0.125 (726457) Bins: 256 Bin Width: 0.250	93.14 s. MSE: 1.0 PSNR: 48.27 dB MS-SSIM: 0.9099

  LABORATOIRE D'INTEGRATION DES SYSTEMES ET DES TECHNOLOGIES	Image restoration by inpainting methods applied to CT reconstruction	Réf : DISC/LITT /11 RT000	34
		DATE: 04 09 2012	49
DISC/LITT	Marcos VARGAS	 Révision	1

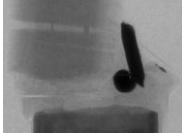

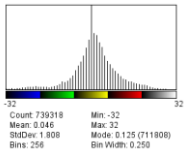
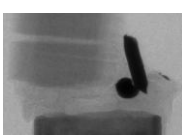

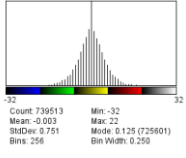
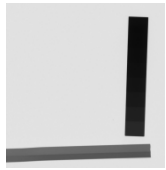
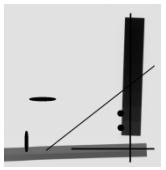
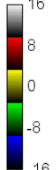



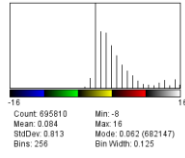
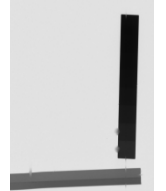
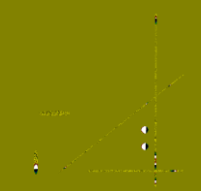
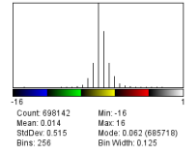
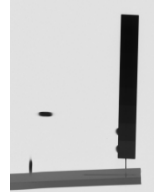

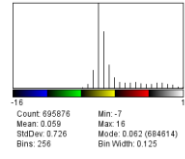


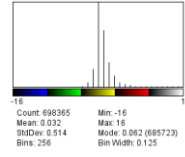
AdB (stopped at 29.7 k iterations)			 Count: 739918 Min: -32 Mean: 0.046 Max: 32 StdDev: 1.808 Mode: 0.125 (711808) Bins: 256 Bin Width: 0.250	80400.59 s. MSE: 2.6 PSNR: 41.57 dB MS-SSIM: 0.8851
Exemplar Based (ExB) patch size: 3 x 3 px.			 Count: 735613 Min: -32 Mean: -0.003 Max: 22 StdDev: 0.751 Mode: 0.125 (725001) Bins: 256 Bin Width: 0.250	576.84 s. MSE: 0.3 PSNR: 50.31 dB MS-SSIM: 0.9201
Inpainting Method	Final Result	Comparative Fig.	Histogram	Image Quality

Figure 5-10. Test on Noisy Images (SkyScan2011). Internal images were cropped to 106 x 69 for visibility.

The best four results were highlighted with blue, and they are: CDD, Euler's Elastica, FMM, and ExB.

				Source: PerkinElmer 821 x 853 px.
TV Rudin			 Count: 695810 Min: -8 Mean: 0.004 Max: 16 StdDev: 0.913 Mode: 0.082 (682147) Bins: 256 Bin Width: 0.125	16.01 s. MSE: 40 PSNR: 31.26 dB MS-SSIM: 0.8626
Curvature Driven Diffusion (CDD)			 Count: 690142 Min: -16 Mean: 0.014 Max: 16 StdDev: 0.515 Mode: 0.082 (685718) Bins: 256 Bin Width: 0.125	43.23 s. MSE: 7 PSNR: 38.82 dB MS-SSIM: 0.9079
MCD			 Count: 695876 Min: -7 Mean: 0.059 Max: 16 StdDev: 0.726 Mode: 0.082 (684614) Bins: 256 Bin Width: 0.125	660.14 s. MSE: 122 PSNR: 26.45 dB MS-SSIM: 0.8787
Euler's Elastica			 Count: 698365 Min: -16 Mean: 0.032 Max: 16 StdDev: 0.514 Mode: 0.082 (685723) Bins: 256 Bin Width: 0.125	89.54 s. MSE: 5.5 PSNR: 39.97 dB MS-SSIM: 0.9039

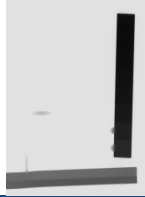
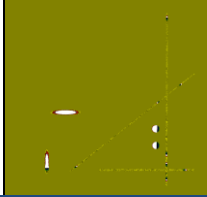
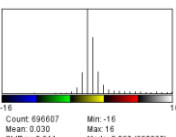

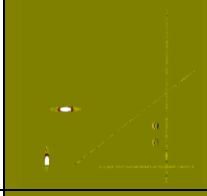
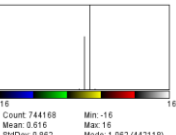
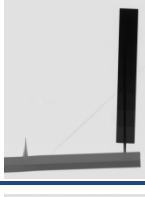
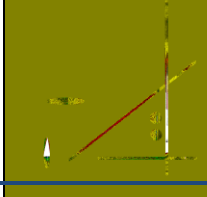
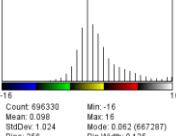
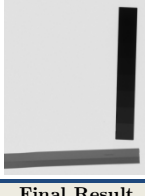

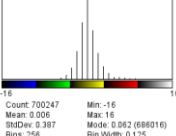
MRI			 Count: 696607 Min: -16 Mean: 0.030 Max: 16 StdDev: 0.644 Mode: 0.062 (685290) Bins: 256 Bin Width: 0.125	23.36 s. MSE: 11 PSNR: 36.77 dB MS-SSIM: 0.8953
FMM			 Count: 744169 Min: -16 Mean: 0.616 Max: 16 StdDev: 0.962 Mode: 0.062 (442118) Bins: 256 Bin Width: 0.125	108.61 s. MSE: 16 PSNR: 36.09 dB MS-SSIM: 0.8998
AdB (stopped at 57.5 k iterations)			 Count: 696530 Min: -16 Mean: 0.098 Max: 16 StdDev: 1.024 Mode: 0.062 (687287) Bins: 256 Bin Width: 0.125	148320.1 s. MSE: 37 PSNR: 31.60 dB MS-SSIM: 0.8619
Exemplar Based (ExB) patch size: 3 x 3 px.			 Count: 700247 Min: -16 Mean: 0.006 Max: 16 StdDev: 0.387 Mode: 0.062 (686016) Bins: 256 Bin Width: 0.125	786.42 s. MSE: 0.2 PSNR: 53.91 dB MS-SSIM: 0.9189
Inpainting Method	Final Result	Comparative Fig.	Histogram	Image Quality

Figure 5-11. Test on Noisy Images (PerkinElmer). Internal images were cropped to 82 x 85 for visibility.

The best four results were highlighted with blue, and they are: CDD, Euler's Elastica, MRI, and ExB.

5.4. Algorithm Optimization and Test on Sinograms

5.4.1. Optimization for Fast Inpainting Execution

In numerical computation, Marquina's algorithm [21] speeds-up the TV Inpainting algorithms. His idea on how to speed up a time marching scheme, consists that weighted steepest descent method generally converges faster than the original one. His idea consists on multiplying internal terms by $|\nabla u|$ with the purpose of reducing stiffness, it is also called *Accelerated Time Marching method* [ATM]. All the results showed during this works, were based on their optimized version.

SkyScan2011 Real Image	Normal Time (s.)	With Marquina Optimization Time (s.)	Optimization in Time by (%)
MCD	222,86	117,78	189,22
Euler's Elastica	109,49	69,74	157,00
MRI	94,81	19,13	495,61

Figure 5-12. Optimization Results.

5.4.1. Semi-automatic Mask Creation

Creating manually a mask is a very long unproductive process. It takes much more time in the Sinogram domain due to its particular form. To solve this, we started from the same image to get its mask version. We converted the Sinogram with artifacts to 8-bit grayscale. Then, we created a 'threshold' binary image. Finally, we used the 'Fill Holes' option from ImageJ. We obtained a good mask within just one iteration of using the previous option (Figure 5-13).

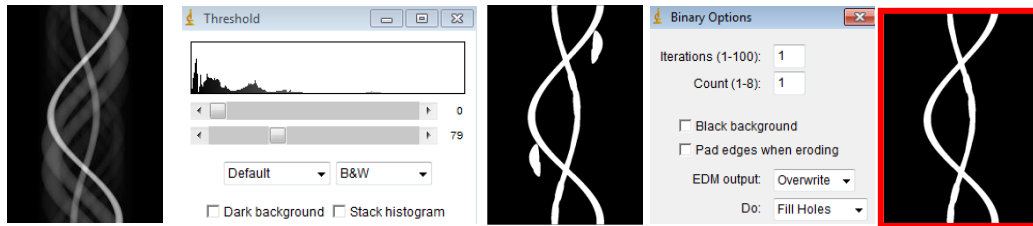

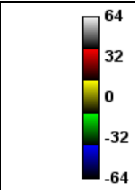
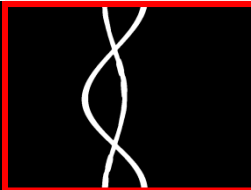

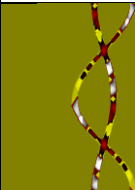
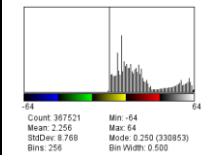
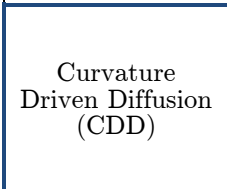
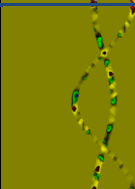
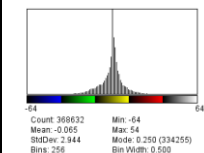
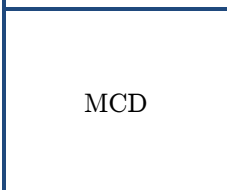
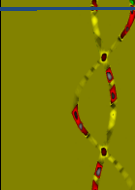
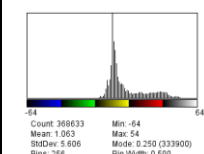
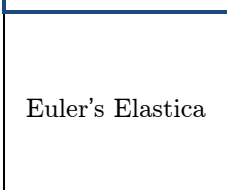
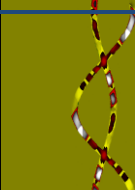
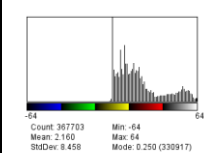





Figure 5-13. Semi-automatic Mask Creation (used in Figure 5-14).

5.4.2. Evaluation on a CT Realistic Synthetic Image from CIVA (noiseless)

				Source: CIVA (Sinogram) 512 x 720 px.
TV Rudin				30.456 s. MSE: 71 PSNR: 20,45 dB MS-SSIM: 0.5849
Curvature Driven Diffusion (CDD)				82.913 s. MSE: 7 PSNR: 30,63 dB MS-SSIM: 0.9218
MCD				540.7510 s. MSE: 24 PSNR: 25,26 dB MS-SSIM: 0.8981
Euler's Elastica				187.6 s. MSE: 67 PSNR: 20,72 dB MS-SSIM: 0.6579

  LABORATOIRE D'INTEGRATION DES SYSTEMES ET DES TECHNOLOGIES	Image restoration by inpainting methods applied to CT reconstruction	Réf : DISC/LITT /11 RT000	37
		DATE: 04 09 2012	49
DISC/LITT	Marcos VARGAS	 Révision	1


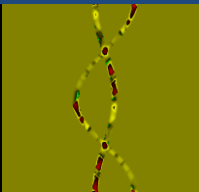
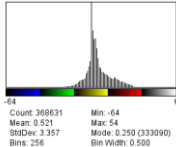

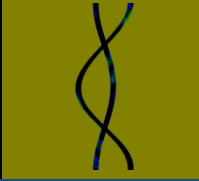
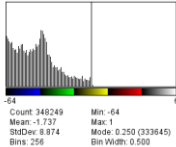


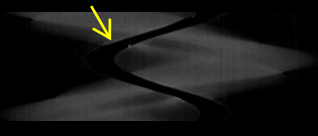
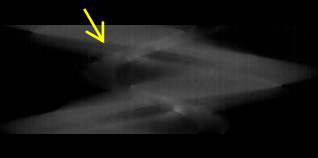
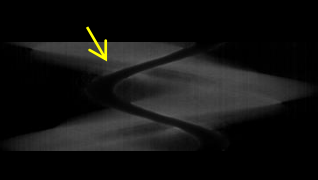
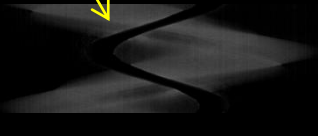
MRI			 Count: 368631 Min: -64 Mean: 0.521 Max: 64 StdDev: 3.357 Mode: 0.250 (333090) Bins: 256 Bin Width: 0.500	50.427 s. MSE: 9 PSNR: 29,67 dB MS-SSIM: 0.9165
AdB (stopped at 11.1 k iterations)			 Count: 340249 Min: -64 Mean: -1.727 Max: 1 StdDev: 8.874 Mode: 0.250 (333645) Bins: 256 Bin Width: 0.500	14178.6 s. MSE: 537 PSNR: 11,68 dB MS-SSIM:
Inpainting Method	Final Result	Comparative Fig.	Histogram	Image Quality

Figure 5-14. Test on Noiseless Sinogram (CIVA). Internal images were cropped to 51 x 72 for visibility.

5.4.3. Evaluation on a CT Real Image from SkyScan2011 (noisy)

Now, we do a qualitative analysis in Figure 5-15, because in this real case we do not have a reference image to quantify the results.

No reference in this EXPERIMENTAL Sinogram			Source: SkyScan2011 (Sinogram) 1280 x 360 px.
TV Rudin		It seems that, it was only filled in with a pure black	32.104 s.
Curvature Driven Diffusion (CDD)		The best result among the 08 inpainting methods	86.023 s.
MCD		Some evidences that the information in the borders is used to fill in.	720.45 2 s.
Euler's Elastica		It seems that, it was only filled in with a pure black	176.175 s.

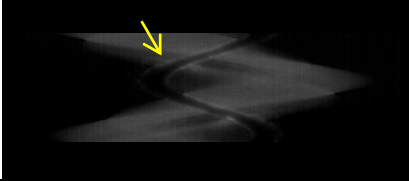
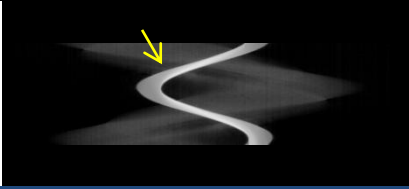
MRI		Strong evidences that the information in the borders is used to fill in.	47.423 s.
AdB (stopped at 5000 iterations)		Even if we wait hours for better results, the improvement won't be significant.	7355.63 seg
Inpainting Method	Final Result	Comparative Fig.	Image Quality

Figure 5-15. Test on experimental Sinogram. Internal images were cropped to 128 x 36 for visibility.

The best qualitative result was highlighted with blue, it was: CDD.

5.5. Choice of the Adapted Algorithm

For the step 1P (Figure 5-7), we take the four best results from Figure 5-9, Figure 5-10 and Figure 5-11 to analyze them simultaneously. The choice will be a balance act between high quality and real-time constraints.

CIVA	Time (s.)	Quality		
		MSE *100	PSNR [dB]	MS-SSIM *100
CDD	9.83	90	48.61	84.39
Euler's Elastica	19.47	30	52.96	84.31
MRI	5.35	50	51.29	84.01
ExB	42.12	10	57.81	98.99
Ideal	0	0	100	100

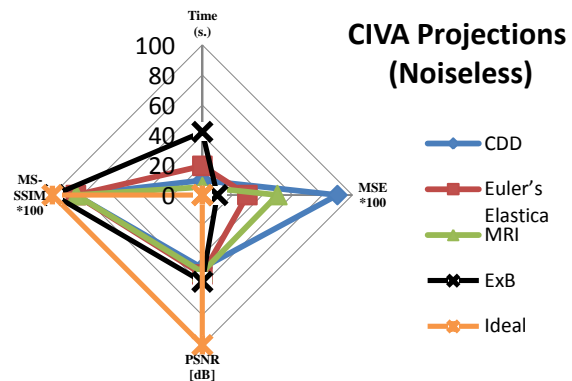


Figure 5-16. Radar chart of the 04 best results of Figure 5-9 (right), detailed table (left).

SkyScan2011	Time (s.)	Quality		
		MSE *100	PSNR [dB]	MS-SSIM *100
CDD	34.14	20	52.98	92.32
Euler's Elastica	69.74	60	48.17	91.85
FMM	93.14	100	48.27	90.99
ExB	576.84	30	50.31	92.01
Ideal	0	0	100	100

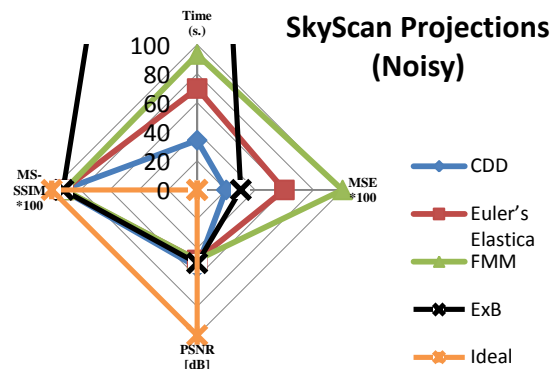


Figure 5-17. Radar chart of the 04 best results of Figure 5-10 (right), detailed table (left).

PerkinElmer	Time (s.)	Quality		
		MSE *10	PSNR [dB]	MS-SSIM *100
CDD	43.23	70	38.82	90.79
Euler's Elastica	89.54	55	39.97	90.39
MRI	23.36	110	36.77	89.53
ExB	786.42	2	53.91	91.89
Ideal	0	0	100	100

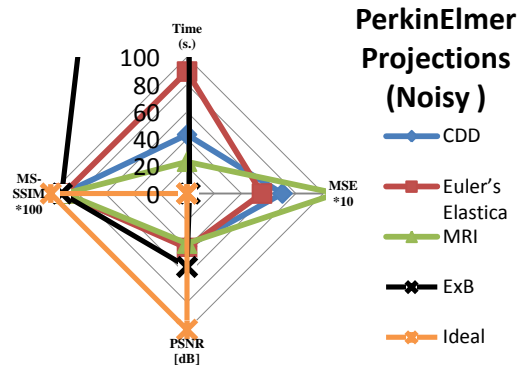


Figure 5-18. Radar chart of the 04 best results of Figure 5-11 (right), detailed table (left).

For the step 2S (Figure 5-7), we take the three best results from Figure 5-14 to analyze them simultaneously. The choice will be a balance act between high quality and real-time constraints. Additionally, the FMM and ExB were shown that do not work in this domain.

Sinogram	Time (s.)	Quality		
		MSE	PSNR [dB]	MS-SSIM *100
CDD	82,913	7	30,63	92,18
MCD	540,751	24	25,26	89,81
MRI	50,427	9	29,67	91,65
Ideal	0	0	0	0

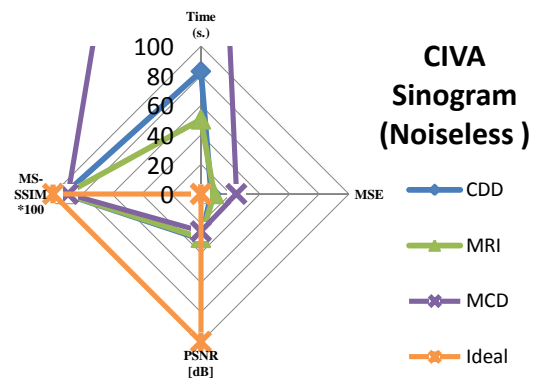


Figure 5-19. Radar chart of the 03 best results of Figure 5-14 (right), detailed table (left).

5.6. Validation on Simple Synthetic Images (noiseless)

The almost fully occlusion on the corners of a square is a challenging problem (Figure 5-20).

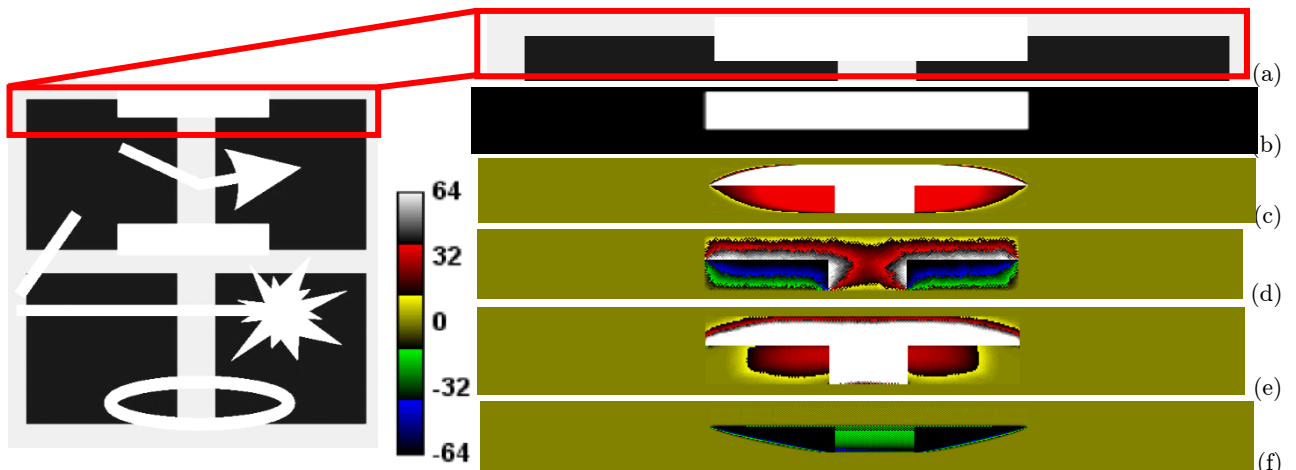


Figure 5-20. Simple Synthetic Image: (a) Region to inpaint zoomed, (b)mask. Zoomed regions of the comparative images using: (c) TV, (d) CDD, (e) Euler's Elastica and (f) AdB.

5.7. Validation on a CT Real Image from PerkinElmer (noisy) in Projection

We evaluated the problem in inpainting circular zones, because lines are quiet well inpainted by most of them. The image results are from Figure 5-11. We arrive into the same results as Xiaoli Huan [22] had for artistic images (in special the one from Telea, FMM [6]).

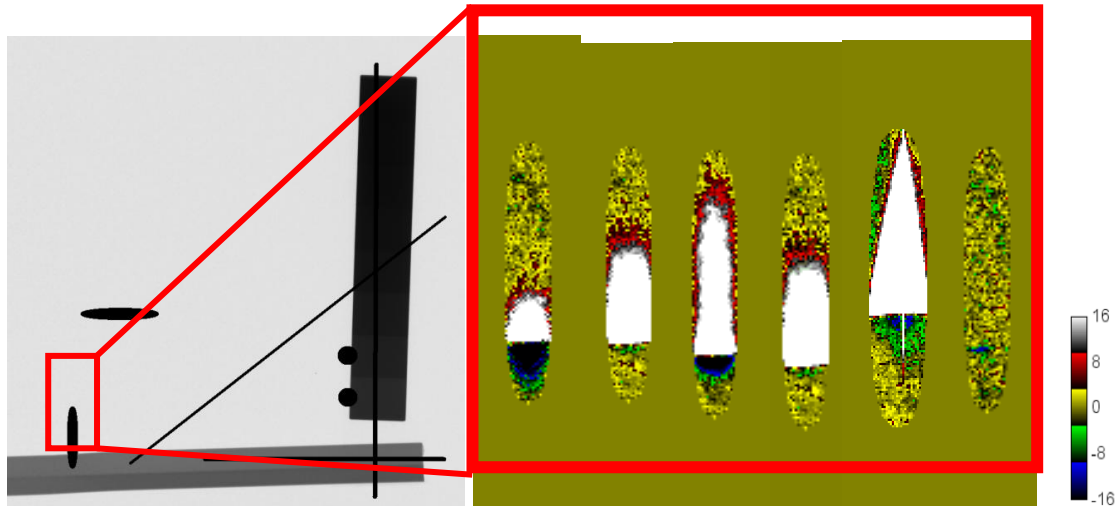


Figure 5-21. Problem in inpainting circular zones. Zoomed comparative images of PerkinElmer (Figure 5-11) using: (a) CDD, (b) Euler, (c) MRI, (d) FMM, (e) AdB, (f) ExB.

5.1. Validation on a CT Realistic Synthetic Image (noiseless) in Sinogram

The Sinogram is a special image, where in some cases the above best algorithms do not work.

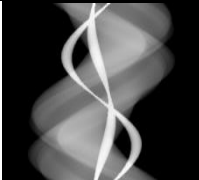

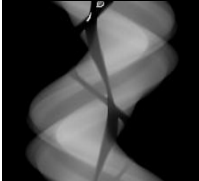
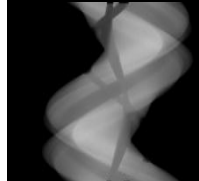
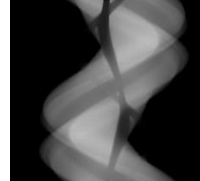
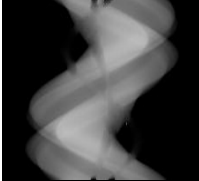
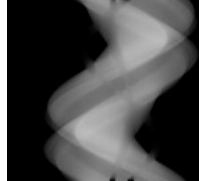

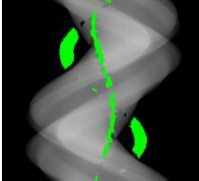



Particular Case		Particular Case			Source: CIVA 256 x 180 px.
TV Rudin		Euler's Elastica		MCD	
Curvature Driven Diffusion (CDD)		MRI		AdB (stopped at 45.5 k iterations)	
Exemplar Based (ExB) patch size: 2 x 2 px.		The part where this algorithm had problems was highlight with green	For this case the algorithm becomes unstable	FMM cannot start	FMM and ExB have problems @ Sinogram
Inpainting Method	Final Result	Comparative Fig.	Histogram	Image Quality	

Figure 5-22. Particular case in the Sinogram domain. Internal images were cropped to 94 x 67 for visibility.

  LABORATOIRE D'INTEGRATION DES SYSTEMES ET DES TECHNOLOGIES	Image restoration by inpainting methods applied to CT reconstruction	Réf : DISC/LITT /11 RT000	41
		DATE: 04 09 2012	49
DISC/LITT	Marcos VARGAS	 Révision	1

Chapter 6

Conclusions and Directions for Future Work

Conclusions




We presented a study in image restoration. We applied eight inpainting methods aiming to reduce the metal artefacts. We gave comparative results on both simulated and experimental CT images, coming from three different sources: CIVA, SkyScan2011, PerkinElmer.

As a general rule, we can say that there is no a 'best method' for all cases. For a decision in a particular image domain, we have to make a balance choice between higher quality and real-time constraints (QT balance). We performed a quantitative analysis by using MSE, PSNR and MS-SSIM index; and qualitative analysis when experimental image do not have a reference.

Our methodology, in one hand, starts at the projection domain [1P]. The zones to inpaint were less than 6% of the total image. First, for the simulated CIVA image (noiseless image), our best inpainting method is ExB (almost perfect). Second, for the noisy images (SkyScan2011, PerkinElmer), the best QT balance is achieved by CDD inpainting method. CDD is 17 times faster than ExB, but its quality could be 35 times less in some cases.

On the other hand, we process also in the sinogram domain [2S]. We did a qualitative and quantitative analysis. In a noiseless Sinogram, there is a QT balance between CDD and MRI, but in its experimental part (SkyScan2011) is the CDD inpainting method the one that is able to start and finish with the best qualitatively result. In this domain FMM and ExB were not able to start, or if so they entered into a search cycle with no improvement in each iteration. In addition, independently of the domain the AdB method (Tschumperle's algorithm [23]), did not give good results for the cases worked in this study. It is computationally expensive and may take few days on an ordinary PC when choosing a high number of iterations.

The mask generation is one key and crucial point in the inpainting. This influences directly in the results. In the case of ExB, the patch size is also crucial. If it is so small, the algorithm will not complete all the process. It will never stop. If it is so big the error will be so evident. A semi-automatic mask (by threshold), for finding the MA without human interaction is specially needed in the sinogram domain.

  LABORATOIRE D'INTEGRATION DES SYSTEMES ET DES TECHNOLOGIES	Image restoration by inpainting methods applied to CT reconstruction	Réf : DISC/LITT /11 RT000	42
		DATE: 04 09 2012	49
DISC/LITT	Marcos VARGAS	 Révision	1

During this work we also try to generate, among the used inpainting methods, an hybrid method that could give us the best part of each one. But, once an algorithm starts working it uses its math propagation definition that will not be compatible for the coming; and if so, then a second mask of smaller unknown form will have to be declared for the second inpainting method to continue. For example, if we combine a TV technique with the texture concept of ExB, then the mask and working procedures will be incompatible.

One important thing to highlight, is that even if there is an 'evolution' in the family of TV inpainting algorithms, it has been proved that in general the best result for our MAR problem is the CDD, in both domains: projection [1P] and sinogram [2S].




Limitations

The time to process the images by inpainting is an important constraint in CT because it uses a high number of images.

Perspectives




First, retest with the latest algorithms published on each family of inpainting methods (since 2009), so that, a new improved comparison could be used for both a fast and better metal artifact reduction. Second, under the context of more general *sparse*¹⁷ image representations (using over complete dictionaries adapted to the representation of image geometry and texture), Elad et al. [24] proposed an image decomposition model with sparse coefficients for the geometry and texture components of the image, and showed that the model can be easily adapted for image inpainting.

¹⁷ Sparse approximation (sparse decomposition) is the problem of estimating a sparse multi-dimensional vector, satisfying a linear system of equations given high-dimensional observed data and a design matrix. [Wikipedia]

  LABORATOIRE D'INTEGRATION DES SYSTEMES ET DES TECHNOLOGIES	Image restoration by inpainting methods applied to CT reconstruction	Réf : DISC/LITT /11 RT000	43
		DATE: 04 09 2012	49
DISC/LITT	Marcos VARGAS	 Révision	1




Bibliography

- [1] S. Masnou, "AP Workshop: Computing in Image Processing, Computer Graphics, Virtual Surgery, and Sports. Conference: Inpainting: a state-of the-art, at IMA (Institute for Mathematics and its Applications)," University of Minnesota, 07-11 March 2011. [Online]. Available: <http://www.ima.umn.edu/videos/?id=1565>. [Accessed 17 August 2012].
- [2] M. Costin, Multiresolution Image Reconstruction in X-ray Micro- and Nano-Computed Tomography: Application in Materials Non-Destructive Testing, CEA-Saclay: Ph.D. Thesis, 2010.
- [3] J. Barrett and N. Keat, "Artifacts in CT: Recognition and Avoidance," *Radiological Society of North America*, vol. 24, pp. 1679 -1691, 2004.
- [4] Y. Li, X. Bao, X. Yin and Y. Chen, "Metal artifact reduction in CT based on adaptive steering filter and nonlocal sinogram inpainting," *3rd International Conference on Biomedical Engineering and Informatics (BMEI 2010)*, vol. 1, no. 4, pp. 380-383 , 2010.
- [5] E. Meyer, R. Raupach, B. Schmidt, A. Mahnken and M. Kachelriess, "Adaptive normalized metal artifact reduction (ANMAR) in computed tomography," in *Nuclear Science Symposium and Medical Imaging Conference (NSS/MIC), 2011 IEEE*, 2011.
- [6] A. Telea, "An image inpainting technique based on the fast marching method," *JOURNAL OF GRAPHICS TOOLS.*, vol. 9, no. 1, pp. 23-34, 2004.
- [7] J. Sethian, *Level Set Methods and Fast Marching Methods: Evolving Interfaces in Computational Geometry, Fluid Mechanics, Computer Vision, and Materials Science on Applied and Computational Mathematics*, (8th Printing) 2nd ed., NY: Cambridge University Press, 2007.
- [8] D. Rachid and F. Olivier, "Les EDP en Traitement des Images et Vision par Ordinateur," INRIA, Sophia-Antipolis, France, 1995.
- [9] L. Rudin and S. Osher, "Total variation based image restoration with free local constraints," vol. 1, no. Proc. 1st IEEE ICIP, pp. 31-35, 1994.
- [10] L. Rudin, S. Osher and E. Fatemi, "Nonlinear total variation based noise removal algorithms," *Physica D*, vol. 60, pp. 259-268, 1992.
- [11] T. Chan and J. Shen, "Non-Texture Inpainting by Curvature-Driven Diffusion (CDD)," *Report UCLA. The University of California, Los Angeles (UCLA), USA.*, vol. 6, no. 2, p. 16, 2000.
- [12] M. Bertalmio, A. Bertozzi and G. Sapiro, "Navier-stokes, fluid dynamics, and image and video

  LABORATOIRE D'INTEGRATION DES SYSTEMES ET DES TECHNOLOGIES	Image restoration by inpainting methods applied to CT reconstruction	Réf : DISC/LITT /11 RT000	44
		DATE: 04 09 2012	49
DISC/LITT	Marcos VARGAS	 Révision	1




inpainting," in *Computer Vision and Pattern Recognition, 2001. CVPR 2001. Proceedings of the 2001 IEEE Computer Society Conference on, 2001.*

- [13] T. Chan and J. Shen, "Euler's Elastica and Curvature Based Inpaintings," *Report UCLA. The University of California, Los Angeles (UCLA), USA.*, vol. 7, no. 11, p. 28, 2001.
- [14] K. Ni, S. Thiruvankadam and T. Chan, "Matting through Variational Inpainting," *IEEE - UCLA. The University of California, Los Angeles (UCLA), USA.*, vol. 6, no. 17, pp. 1-13, 2008.
- [15] C. Brito-Loeza and K. Chen, "Fast Numerical Algorithms for Euler's Elastica Inpainting Model," *International Journal of Modern Mathematics*, vol. 5, no. 2, pp. 157-182, 2010.
- [16] T. Chan and J. Shen, "Morphological Invariant PDE Inpaintings," *Report UCLA. The University of California, Los Angeles (UCLA), USA.*, vol. 6, no. 9, p. 14, 2001.
- [17] D. Tschumperle and R. Deriche, "Vector-valued image regularization with PDEs: A common framework for different applications," *Pattern Analysis and Machine Intelligence, IEEE Transactions on*, vol. 27, no. 4, pp. 506-517, 2005.
- [18] A. Criminisi, P. Perez and K. Toyama, "Object Removal by Exemplar-Based Inpainting," *IEEE Computer Society Conference on Computer Vision and Pattern Recognition (CVPR'03)*, no. 1063-6919/03, p. 8, 2003.
- [19] R. Fernandez, S. Legoupil, M. Costin, D. Tisseur and A. Leveque, "CIVA Computed Tomography Modeling," in *18th World Conference on Nondestructive Testing, Durban, South Africa, 2012.*
- [20] Z. Wang, A. Bovik, H. Sheikh and E. Simoncelli, "Image quality assessment: From error visibility to structural similarity," *Image Processing, IEEE TRANSACTIONS ON IMAGE PROCESSING*, vol. 13, no. 4, pp. 600-612, 2004.
- [21] A. Marquina and S. Osher, "Explicit algorithms for a new time dependent model based on level set motion for nonlinear deblurring and noise removal," *SIAM Journal on Scientific Computing*, vol. 22, no. 4, pp. 387-405, 2000.
- [22] A. X. Huan, B. Murali and A. Ali, "Image restoration based on the fast marching method and block based sampling," *Computer Vision and Image Understanding*, vol. 114, no. 8, pp. 847 - 856, 2010.
- [23] D. Tschumperle and R. Deriche, "Vector-valued image regularization with PDEs: A common framework for different applications," *Pattern Analysis and Machine Intelligence, IEEE Transactions on*, vol. 27, no. 4, pp. 506--517, 2005.
- [24] M. Elad, J. Starck, P. Querre and D. Donoho, "Simultaneous cartoon and texture image inpainting using morphological component analysis (MCA)," *Applied and Computational Harmonic Analysis*, vol. 19, p. 340-358, 2005.
- [25] T. Buzug, *Computed Tomography - From Photon Statistics to Modern Cone-Beam CT*, 1st ed., Berlin: Springer - Verlag Berlin Heidelberg, 2008.

  LABORATOIRE D'INTEGRATION DES SYSTEMES ET DES TECHNOLOGIES	Image restoration by inpainting methods applied to CT reconstruction	Réf : DISC/LITT /11 RT000	45
		DATE: 04 09 2012	49
DISC/LITT	Marcos VARGAS	 Révision	1

[26] K.-Y. Ni, Variational PDE-based Image Segmentation and Inpainting with Applications in Computer Graphics, University of California, Los Angeles: Ph.D. thesis, 2008.

[27] A. Bugeau, M. Bertalmio, C. Vicent and S. Guillermo, "A Unifying Framework for Image Inpainting," *Institute for Mathematics and its Applications (IMA), USA*, vol. IV, no. 6, 2009.

  LABORATOIRE D'INTEGRATION DES SYSTEMES ET DES TECHNOLOGIES	Image restoration by inpainting methods applied to CT reconstruction	Réf : DISC/LITT /11 RT000	46
		DATE: 04 09 2012	49
DISC/LITT	Marcos VARGAS	 Révision	1

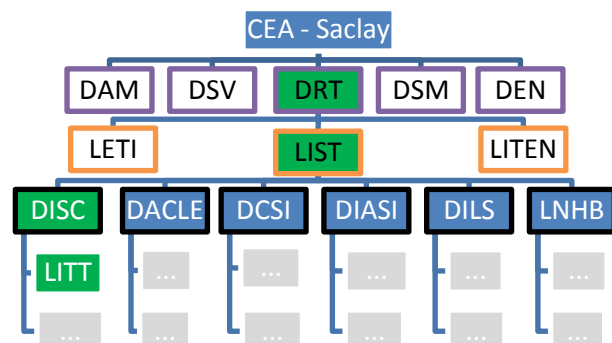
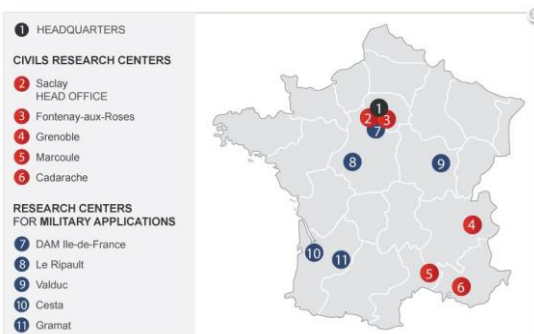
Appendix 1

CEA: Atomic Energy and Alternative Energies Commission






CEA is divided into 5 directions, or divisions:

1. Direction de l'énergie Nucléaire - DEN (Christophe Behar).
2. Direction des Applications Militaires - DAM (Daniel Verwaerde), which builds the nuclear weapons of the French military and designs the power plants of the nuclear submarines of the French Navy [picture on the right side].
3. Direction des Sciences de la Matière - DSM (Gabriele Fioni).
4. Direction des Sciences du Vivant - DSV (Gilles Bloch).
5. **Direction de la Recherche Technologique - DRT (Jean Therme)**
 - 5.1. LETI, Laboratoire d'Electronique et de Technologie de l'Information.
 - 5.2. LITEN, Laboratoire d'Innovation pour les Technologies des Energies nouvelles et les Nanomatériaux.
 - 5.3. **LIST, Laboratoire d'Intégration des Systèmes et des Technologies.**
 - 5.3.1. DACLE - Département Architecture, Conception et Logiciels Embarqués.
 - 5.3.2. DCSI - Département Capteurs, Signal et Information.
 - 5.3.3. DIASI - Département Intelligence Ambiante et Systèmes Interactifs.
 - 5.3.4. DILS - Département Ingénierie Logiciels et Systèmes.
 - 5.3.5. LNHB - Laboratoire National Henri Becquerel.
 - 5.3.6. **DISC - Département Imagerie Simulation pour le Contrôle.**
 - 5.3.6.1. **LITT – Laboratoire Image, Tomographie et Traitements.**



CEA-Saclay: (a) HQ and other related centers in France, (b) simplified organization.

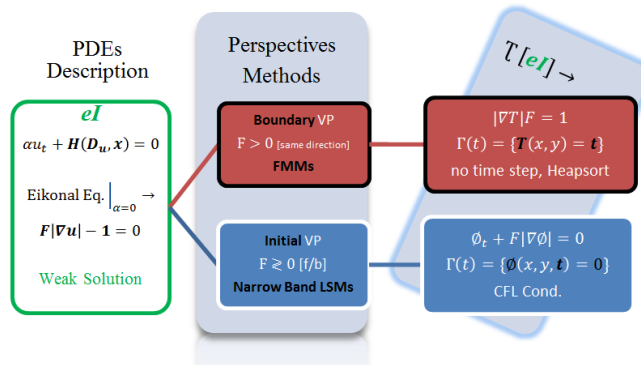
  LABORATOIRE D'INTEGRATION DES SYSTEMES ET DES TECHNOLOGIES	Image restoration by inpainting methods applied to CT reconstruction	Réf : DISC/LITT /11 RT000	47
		DATE: 04 09 2012	49
DISC/LITT	Marcos VARGAS	 Révision	1

Appendix 2

Level Set Methods (LSMs) vs Fast Marching Methods (FMMs): Similarities & Differences.

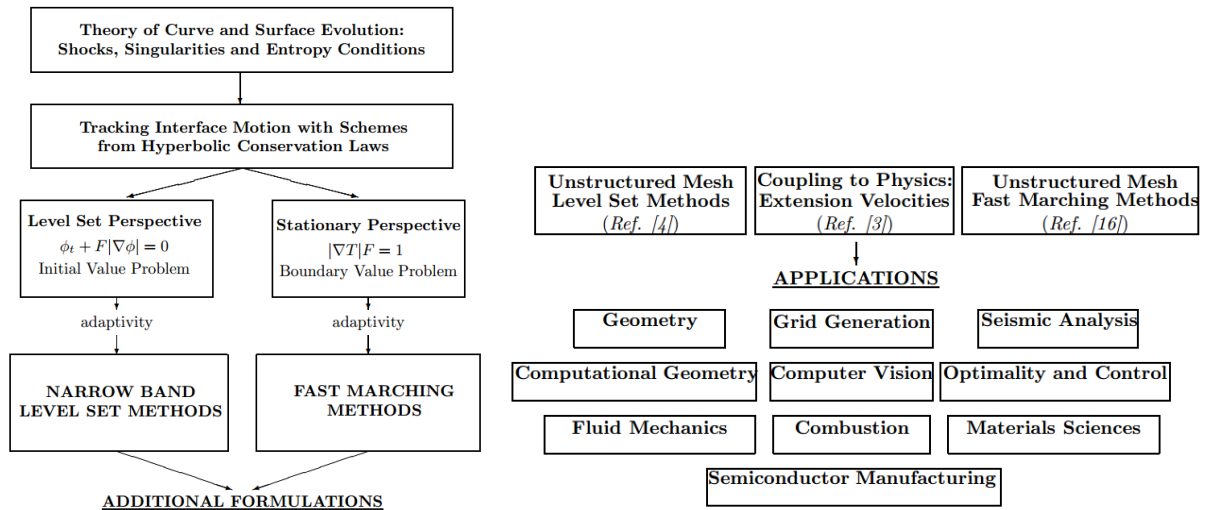
1. *Unchanged in N-Dimensions.*
 2. *Break/Merge Topologically: T, Φ remain single-valued.*
 3. *Rely on viscosity solutions: an **entropy** weak solution*
 4. *Numerical solutions of Hyperbolic Conservation Law.*
- $$\Phi(ih, jh, n\Delta t) \rightarrow -\frac{\Phi_{ij}^{n+1} - \Phi_{ij}^n}{\Delta t} + F|\nabla_{ij}\Phi_{ij}^n| = 0$$
5. *Intrinsic Geometric Properties: Normal \vec{n} , Curvature κ*
 6. *Used **Adaptive Computational Strategies**.*



Similarities:



Differences:

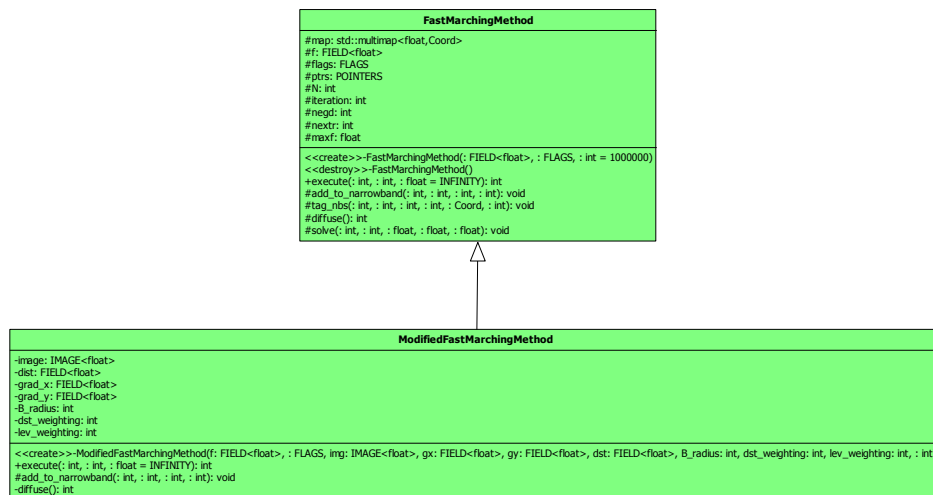
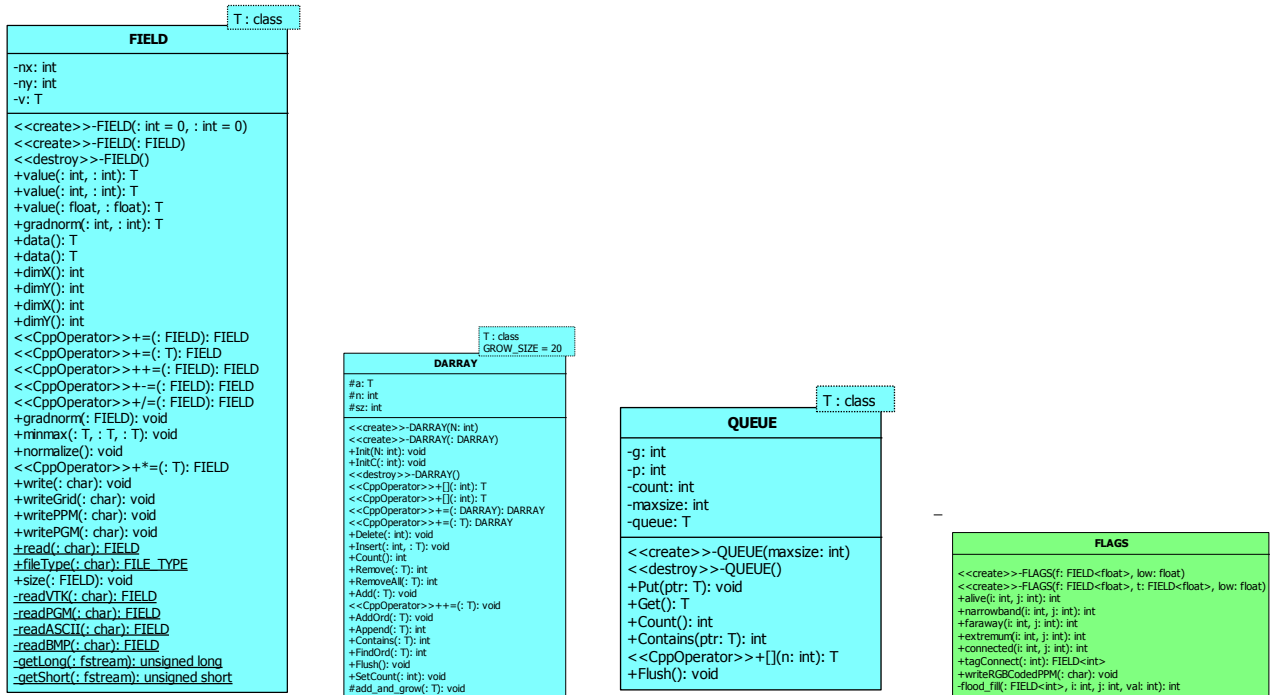
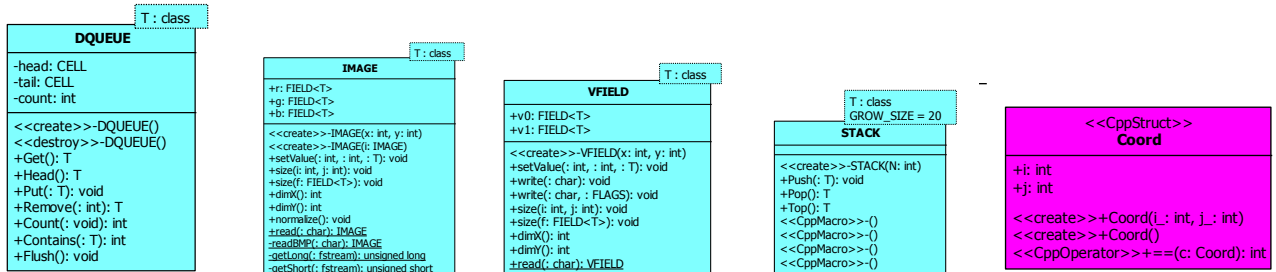
Algorithms and applications for interface propagation (eI) [7] :






 list LABORATOIRE D'INTEGRATION DES SYSTEMES ET DES TECHNOLOGIES	Image restoration by inpainting methods applied to CT reconstruction	Réf : DISC/LITT /11 RT000	48
		DATE: 04 09 2012	49
DISC/LITT	Marcos VARGAS	 Révision	1

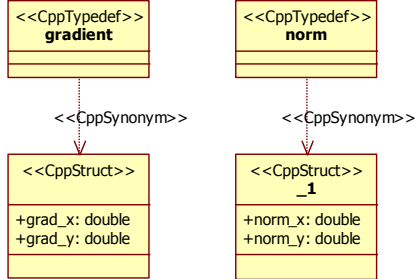
Appendix 3 FMM and ExB. UML classes used.

FMM



  LABORATOIRE D'INTEGRATION DES SYSTEMES ET DES TECHNOLOGIES	Image restoration by inpainting methods applied to CT reconstruction	Réf : DISC/LITT /11 RT000	49
		DATE: 04 09 2012	49
DISC/LITT	Marcos VARGAS	 Révision	1

ExB



inpainting
+m_pImage: CImage +m_bOpen: bool +m_width: int +m_height: int +m_color: COLORREF +m_r: double +m_g: double +m_b: double +m_top: int +m_bottom: int +m_left: int +m_right: int +m_mark: int +m_confid: double +m_pri: double +m_gray: double +m_source: bool
<<create>>-inpainting(name: char) <<destroy>>-inpainting(: void) +process(: void): bool +DrawBoundary(: void): void +ComputeConfidence(i: int, j: int): double +priority(x: int, y: int): double +ComputeData(i: int, j: int): double +Convert2Gray(: void): void +GetGradient(i: int, j: int): gradient +GetNorm(i: int, j: int): norm +draw_source(: void): bool +PatchTexture(x: int, y: int, patch_x: int, patch_y: int): bool +update(target_x: int, target_y: int, source_x: int, source_y: int, confid: double): bool +TargetExist(: void): bool +UpdateBoundary(i: int, j: int): void +UpdatePri(i: int, j: int): void

CImage
+m_hDib: HANDLE +m_bIsAttached: BOOL +m_pBMI: LPBITMAPINFO +m_pPixel: LPBYTE +m_WidthBytes: LONG +m_BMPwidth: LONG +m_BMPheight: LONG
<<create>>-CImage() <<create>>-CImage(hDib: HANDLE) <<create>>-CImage(width: LONG, height: LONG, bitCount: WORD) <<destroy>>-CImage() +Convert2Gray(pDestImg: CImage): void +Save(lpszFilePath: LPCTSTR, pData: LPBYTE): BOOL +Draw(hDC: HDC, ptOriginDst: POINT, sizeDst: SIZE, rcSrc: RECT): BOOL +Mirror(): BOOL +Negate(): BOOL +HLStoRGB(H: double, L: double, S: double): COLORREF +HueToRGB(m1: double, m2: double, h: double): double +RGBtoHSL(rgb: COLORREF, H: double, S: double, L: double): void +SetPixel(x: int, y: int, value: COLORREF): BOOL +GetBitsPerPixel(): int +GetPixel(x: int, y: int, value: COLORREF): BOOL +Lock(): BOOL +Unlock(): BOOL +BMI(): LPBITMAPINFO +Pixel(): LPBYTE +Width(): LONG +Height(): LONG +Size(): LONG +WidthBytes(): LONG +Get(x: LONG, y: LONG): BYTE +Put(x: LONG, y: LONG, byPixel: BYTE): VOID +Ptr(x: LONG, y: LONG): LPBYTE +GetRGB(x: LONG, y: LONG): RGBTRIPLE +PutRGB(x: LONG, y: LONG, rgbPixel: RGBTRIPLE): VOID +PtrRGB(x: LONG, y: LONG): RGBTRIPLE +Create(width: LONG, height: LONG, bitCount: WORD): BOOL +Release(): VOID +Attach(hDib: HANDLE): BOOL +Detach(): HANDLE +Clear(byInit: BYTE): VOID +Gaussian(pDest: CImage): BOOL +GaussianRGB(pDest: CImage): BOOL +Copy(pDestDIB: CImage): VOID +Draw(hDC: HDC, x: LONG, y: LONG): VOID +Stretch(hDC: HDC, x: LONG, y: LONG, width: LONG, height: LONG): VOID +Load(lpszFilePath: LPCTSTR): BOOL +Save(lpszFilePath: LPCTSTR): BOOL +AddToFileEnd(pfile: FILE): BOOL +LoadFromCurPos(pfile: FILE): BOOL +ConvertToGray(): HANDLE +ExtractChannel(cFlag: char): HANDLE +BilinearZoomIn(ratio: int): HANDLE +GetPSNRColor(pRecon: CImage, iBW: int, iBH: int): double +GetPSNRGray(pRecon: CImage, iBW: int, iBH: int): double +TransToYIQ(): CImage -CombineYIQ(pYData: float, pIData: float, pQData: float): CImage -GetYIQ(pYData: float, pIData: float, pQData: float): BOOL #GetColorEntries(pBMI: LPBITMAPINFO): LONG